

國立交通大學  
光電工程研究所  
碩士學位論文

新類波長可調 L-band 鎖模光纖雷射

Novel Wavelength-Tunable L-band  
Mode-Locked Fiber Laser



研究生：張峻源

指導教授：林恭如

中華民國九十五年六月

新類波長可調 L-band 鎖模光纖雷射

**Novel Wavelength-Tunable L-band Mode-Locked Fiber Laser**

研究生：張峻源

Student : Jun-Yuan Chang

指導教授：林恭如 老師

Advisor : Gong-Ru Lin

國立交通大學

光電工程研究所



A Thesis

Submitted to Institute of Electronics College of Engineering  
National Chiao Tung University  
in partial Fulfillment of the Requirements  
for the Degree of  
Master  
In Electro-Optical Engineering

June 2006

Hsinchu, Taiwan, Republic of China

中華民國九十五年六月

# ABSTRACT

Title : A Power Conversion Efficiency Improved L-Band Erbium-Doped Fiber Laser with Coupling-Ratio Controlled Wavelength Tunability

Pages : 1 Page

School : National Chiao Tung University

Department : Institute of Electro-Optical Engineering

Time : June, 2006

Degree : Master

Researcher : Jun-Yuan Chang

Advisor : Prof. Gong-Ru Lin

Keywords : Erbium-Doped Fiber Amplifier, Power Conversion Efficiency, Erbium-Doped Fiber Laser, Mode-Locked Fiber Laser, dispersion compensation.

In this thesis, we study the L-band erbium-doped fiber amplifier (EDFA) and wavelength-tunable erbium-doped fiber laser (EDFL), and further accomplish mode-locked EDFL. An extremely high power conversion efficiency (PCE) of 37% (10% improvement as compared to that reported using conventional L-band EDFA configuration) in the optimized configuration of EDFA is obtained. In wavelength-tunable EDFL, the wavelength shifting phenomenon results from the different intracavity loss by adjusting the output coupling ratio with a tunable-ratio optical coupler (TROC). In the tuning range, covering the whole L-band, the EDFL has extremely high output power and quantum efficiency. Besides, the lasing linewidth of the EDFL output becomes narrower by simply inserting a tiny air-gap between the FC/PC connectors of fiber patch cord, which functions as an intra-cavity Fabry-Perot filter in the cost-effective L-band EDFL system. Then the wavelength tuning of mode-locked EDFL is achieved by adjusting the output coupling ratio with a TROC which introduces wavelength-dependent cavity loss as well as changing the peak of the gain profile. And we also add a tunable band-pass filter in the cavity to attain wavelength-tuning. Finally, according to the dispersion compensation theory, we use single mode fiber with negative group velocity dispersion (GVD) to compress the mode-locked EDFL output with a positively chirped pulse.

# ACKNOWLEDGEMENT

在這兩年的碩士生涯中，首先要特別對我的指導教授 林恭如老師在研究的過程中不斷的給予支持與耐心的指導表達敬意與感謝之意，使我在求學態度受益良多。

感謝實驗室張詠誠、林俊榮、廖育聖、吳銘忠、邱奕祥、林齊冠與陳家陽學長對我不厭其煩的教導，及與我同甘共苦的林螢聰同學在實驗與課業研究上給予的協助，在遇到挫折時給我的最大支持與鼓勵，另外感謝學弟游昆傑在實驗上的協助。最後我要感謝我最摯愛的家人和女友，尤其是在背後默默支持我的父母親，以及其他的好朋友，對於你們全力的支持與關愛，僅致上無限的敬意與感激。



# CONTENTS

	<b>Page</b>
<b>Abstract (in Chinese)</b>	i
<b>Abstract (in English)</b>	ii
<b>Acknowledgement</b>	iii
<b>Contents</b>	iv
<b>List of Figures</b>	vi
<b>Chapter 1 : Introduction</b>	
1.1 L-band EDFA	1
1.2 Tunable L-band EDFL	2
Review of tuning technology	3
1.3 Motivation and chapter description	4
1.4 References	5
<b>Chapter 2 : A power conversion efficiency improved L-band erbium-doped fiber amplifier</b>	
2.1 Introduction	11
2.2 Experimental setup	12
2.3 Principle of 1580-nm Band Amplification	13
2.4 Results and discussions	14
Characteristics of optimized configuration	14
2.5 Conclusions	16
2.6 References	17
<b>Chapter 3 : A coupler and air-gap etalon controlled high-efficiency L-band erbium-doped fiber laser</b>	
3.1 Introduction	21
3.2 Theory of wavelength shifting phenomenon	22
3.3 Experimental setup	24
3.4 Results and discussions	25
Effect of output coupling ratio	26
Effect of total intracavity loss	27
Effect of air-gap	29
3.5 Conclusions	30
3.6 APPENDIX A	30
3.7 References	32
<b>Chapter 4 : Wavelength-tuning mode-locked L-band erbium-doped</b>	

<b>fiber laser by controlled output-coupling-ratio</b>	
4.1 Introduction	35
4.2 Experimental setup	36
4.3 Results and discussions	37
Mode-locked EDFL with TBPF	37
Mode-locked EDFL without TBPF	38
Linear compression of ML-EDFL without TBPF	41
Comparison	43
4.4 Conclusions	44
4.5 References	45
<b>Chapter 5 : Summary</b>	
5.1 Summary	47
<b>Curriculum Vitae</b>	48
<b>Publication list</b>	49



# LIST OF FIGURES

- Fig. 2.1 The schematic diagram of the L-band EDFA.....
- Fig. 2.2 Energy level diagram of the  $\text{Er}^{3+}$  ion. (After Ref. [22]).....
- Fig. 2.3 Schematic diagram of 1580-nm band amplification. (After Ref. [22]).....
- Fig. 2.4 Gain and loss coefficient and ESA cross section of  $\text{Er}^{3+}$ -doped fiber. (After Ref. [22]).....
- Fig. 2.5 Output ASE spectrum of the L-band EDFA.
- Fig. 2.6 Small-signal gain of the EDFL at input signal power of -20 dBm.
- Fig. 3.1 Scheme of the unidirectional EDFL (after Ref. [12]).....
- Fig. 3.2 The schematic diagram of the L-band EDFL. A coupling-ratio controlled wavelength tunable L-band EDFL with a tunable-ratio optical coupler (TROC). .....
- Fig. 3.3 The trend of lasing wavelength, output power, and quantum efficiency with detuning output coupling ratio.
- Fig. 3.4 The lasing spectra of L-band EDFL with detuning output coupling ratio.
- Fig. 3.5 Wavelength dependent output power at 90% output coupling ratio.
- Fig. 3.6 Power stability of the L-band EDFL measured within 10 minutes.
- Fig. 3.7 The lasing linewidth without (solid square) or with (hollow circle) an air-gap inserting between FC/PC fiber connectors.

- Fig. 3.8 The variation of the 3-dB spectral linewidth when the spacing of air-gap is detuned.
- Fig. 4.1 Schematic diagram of the mode-locked EDFL with a TROC-based wavelength tuning configuration.
- Fig. 4.2 The peak power and FWHM pulsewidth of the pulses at output coupling ratio of 10%, 50%, and 90%.
- Fig. 4.3 The 3-dB spectral linewidth and central wavelength of the output EDFL spectra as the output coupling ratio detunes from 10% to 90%.
- Fig. 4.4 The peak power and the pulsewidth of the pulses as the output coupling ratio is adjusted from 10% to 90%. Inset: The autocorrelation traces of the output pulses.
- Fig. 4.5 RF spectrum of the output pulses at 1599.3 nm under 10% output coupling ratio.
- Fig. 4.6 Spectra before and after adding the SMF.
- Fig. 4.7 Variation of pulsewidth by adding different length of the SMF from 22.5 m to 37.5 m. Inset: The autocorrelation traces of the output pulses before and after adding SMF at 10% output coupling ratio.
- Fig. 4.8 The autocorrelation traces of the output pulses after adding 32.5 m SMF at 10%, 50%, and 90% output coupling ratio.
- Table 2.1 Power conversion efficiency (PCE) and the maximum gain of the EDFA pumped at different forward/backward schemes.
- Table 4.1 Comparison of the tuning range, the narrowest pulsewidth, and timing jitter in three different situations.



# Chapter 1

## Introduction

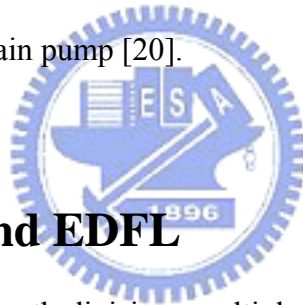
### 1.1 L-band EDFA

Long-wavelength-band erbium-doped fiber amplifiers (L-band EDFAs) have been developed rapidly following the conventional 1550-nm-band (C-band) EDFA as a key component for wavelength division multiplexing (WDM) transmission systems, which made it possible to transmit several terabit per second [1], [2]. Though the gain region of EDFAs is wider than 100 nm, EDFAs using only about 30-nm bandwidth in the C-band were developed in the first few years. With the enhancement of the erbium-doped fiber (EDF) and pump laser diode (LD) manufacturing technology, and also the need for more optical bandwidth in optical communications, the EDFA for the L-band with another optical bandwidth between 1570 and 1600 nm has been developed [3], [4].

The application of the L-band EDFA to WDM transmission systems is very attractive because the system capacity can be doubled when used in conjunction with the conventional C-band EDFA as in-line repeaters [5]. Using dispersion-shifted fibers, it is also possible to construct effective WDM systems with narrow channel spacing of less than 100 GHz without the degradation caused by nonlinear effects, such as four-wave mixing and cross-phase modulation [6], [7]. Moreover, the EDFA without gain-flattening filters can achieve flat gain easier than the C-band EDFA [8], [9].

The relatively low efficiency of the EDFA operating at wavelengths far from the emission peak around 1530 nm has led various efforts to improve the amplification characteristics of the L-band EDFA. The selection of a proper pump wavelength or a

suitable pumping configuration has been one of the main issues [4], [10], [11]. The pump wavelength dependence of the amplification characteristics of the EDFA has been reported mainly in 800-, 980-, and 1480-nm bands, and now the 980- and 1480-nm bands, are mostly used for the L-band EDFA [12]–[14]. On the other hand, the 1555-nm wavelength had been examined as a pump wavelength but it was reported that noise figures were detrimental and gains did not have merits [15], [16]. Lately, the 1555-nm distributed feedback LD was also investigated as a subsidiary pump with a 980- or a 1480-nm band pump and there was a 20% improvement of gain coefficient for a single channel input [17]. Besides, amplified spontaneous emission (ASE) from a pumped EDF was reused as a subsidiary pump employing reflectors or additional EDFs [18], [19], and also the ASE from the pre-amplifier of a 980-nm-pumped EDFA was used with a 1480-nm main pump [20].



## **1.2 Tunable L-band EDFA**

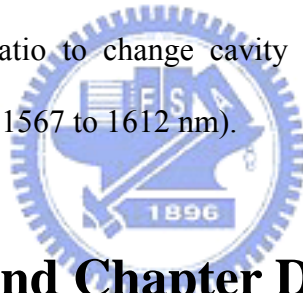
The popularity of wavelength-division multiplexed systems in long-haul optical communications has stimulated a large demand for an enormous number of practical applications for optical components and WDM devices. In recent years, the long wavelength band (L-band) erbium-doped fiber amplifiers have been widely used in WDM systems [21]. That doubled the available bandwidth of optical fiber communications. Testing of such WDM systems and a large number of optical devices requires wavelength-tunable laser sources with spectral range covering the (C+L)-band. Another important application of tunable lasers is in inventory management, where a large number of lasers with different fixed wavelengths are used as transmitter backup for WDM systems. The availability of low-cost and tunable single-wavelength lasers would help to reduce the inventory substantially. Erbium-doped fiber lasers

(EDFLs) have been studied extensively as a very promising solution because they offer several advantages over semiconductor lasers, which include inherent compatibility with optical fiber networks (and hence low insertion loss), high conversion efficiency, ease of construction, and low cost. Fiber lasers based on nonlinear effects are also possible, but they need a much higher input pump power due to the poor conversion efficiency. This problem can be solved by using highly doped EDF to reduce fiber length and decrease pumping power.

Such lasers have been built in the C-band (1529-1565 nm) with erbium-doped fibers by inserting various intracavity comb filters into both linear and ring cavities [22-29]. Previous results have shown that stable C-band multiwavelength oscillation can be achieved by cooling an EDF to the liquid nitrogen temperature [26], by using multiple-core EDF [27], by inserting a frequency shifter [28], or by combining the Brillouin gain and EDF gain [29]. Recent advances have also shown that EDFs can offer L-band gain in the wavelength range between 1568 and 1610 nm [19, 30]. Thus, tunable EDFLs pumped with a 980/1480 nm semiconductor laser diode have been demonstrated with continuously tuning range of over 100 nm [3]–[33], which covers the entire (C + L)-band, and caters for the increased bandwidth requirement in WDM systems, where the C-band and L-band EDFAs are used simultaneously. These lasers may also provide other advantages such as low threshold, high optical signal-to-noise ratio (OSNR), and narrow linewidth.

Several techniques exist to widely tunable fiber lasers, and many of them are based on bulky and expansive optical elements such as C+L band (1520-1600 nm) tunable optical band-pass filters (OBPFs) or wavelength-selective gratings [34]. Typically, three different types of OBPFs including dielectric, grating, and fiber Fabry-Perot (FFP) filters were extensively employed. The dielectric filter is the most common one with a

tunable range limited to 40 nm. The grating filter was comprehensively used in tunable external-cavity laser diode systems with a widely tunable range over 100 nm, however, it has a large polarization dependency and a large splicing loss of >5 dB) during fiber coupling. Among these conventional OBPFs, the FFP filter is an all-fiber based device having a most wide tuning range of >100 nm, a relatively low loss of <2 dB and a extremely low polarization dependence of 0.1 dB [35]. It is preferable to have an all-fiber laser cavity architecture since which exhibits the advantages air-gap free, robust and easily connectable, reliable and potentially cost-effective. Previously, the vintage L-band EDFLs with the wavelength tunability have been shown via the use of fiber Bragg gratings (FBGs), tunable from 1571-1604 nm) [8] or the adjustment on cavity loss (tunable from 1587 to 1606 nm) [9]. Oppositely, our proposed scheme manipulates the coupling ratio to change cavity loss and to cover the full L-band wavelength tunability (from 1567 to 1612 nm).



## 1.3 Motivation and Chapter Description

The broadband optical communication is becoming one of the most promising technologies in the data transmission. The bandwidth is gradually and strongly requested while the triple-play service is delivered to people's daily life. To increase transmission capacity and meet this request for the broadband communication networks, the technologies of the WDM and the optical amplifier are two most attractive technologies. Meanwhile, the Erbium-doped fiber amplifier is the potential optical amplifier today. However, as mentioned previously, the nature, input-dependent gain, of the EDFA will limit the applications in the WDM optical networks. Therefore, how to establish a cost-efficient and high efficient long-wavelength band (L-band) EDFA is an important and valuable research. In

addition, wideband tunable erbium-doped fiber lasers (EDFL) have attracted significant interest for loss measurements of optical components, optical sensing systems, and tunable transmitters in dense wavelength division multiplexing (DWDM) systems. Due to the complicated configurations of wideband tunable EDFL and inspiring of M. Melo et al.'s special method which is depend on cavity loss by fiber taper [36], we have proposed and demonstrated a L-band (1565-1610 nm) fiber laser by using cost-effective methods for the experimental operation. In addition, we also accomplish wideband mode-locked EDFL at repetition of 1GHz and obtain ultrashort pulses by linear compression.

The Thesis is separated five chapters. Chapter 1 is historical review of L-band erbium-doped amplifiers (EDFA) and tunable L-band erbium-doped fiber lasers (EDFL), and motivation. Chapter 2 describes the optimized pumping scheme to obtain high power conversion efficiency for L-band EDFA. Chapter 3 discusses the influence of cavity loss by adjusting output coupling ratio in L-band EDFL. By using this method, we can demonstrate wideband tuning L-band EDFL. Chapter 4 introduces 1 GHz wideband-tuning mode-locked erbium-doped fiber laser. At last, Chapter 5 concludes the experimental results.

## 1.4 References

- [1] S. Bigo, Y. Frignac, G. Charlet, W. Idler, S. Borne, H. Gross, R. Dischler, W. Poehlmann, P. Tran, C. Simonneau, D. Bayart, G. Veith, A. Jourdan, and J. Hamaide, "10.2 Tbit/s ( $256 \times 42.7$  Git/s PDM/WDM) transmission over 100 km TeraLight fiber with 1.28 bit/s/Hz spectral efficiency," in *Proc. OFC2001, Tech. Dig.*, Anaheim, CA, 2001, paper PD25.
- [2] T. Ono and Y. Yano, "Key technologies for terabit/second WDM systems with

- high spectral efficiency of over 1 bit/s/Hz,” *IEEE J. Quantum Electron.*, vol. 34, pp. 2080–2088, Nov. 1998.
- [3] H. Ono, M. Yamada, T. Kanamori, and Y. Ohishi, “Gain-flattened Er -doped fiber amplifier for a WDM signal in the 1.57–1.60  $\mu\text{m}$  wavelength region,” *IEEE Photon. Technol. Lett.*, vol. 9, pp. 596–598, May 1997.
- [4] H. Ono, M. Yamada, T. Kanamori, S. Sudo, and Y. Ohishi, “1.58  $\mu\text{m}$  band gain-flattened erbium-doped fiber amplifiers for WDM transmission systems,” *J. Lightwave Technol. Lett.*, vol. 17, no. 3, pp. 490–496, 1999.
- [5] Y. Sun, J. W. Suhoff, A. K. Srivastavas, A. Abramov, T. A. Strasser, P. F. Wysocki, J. R. Pedrazzani, J. B. Judkins, R. P. Espindola, C. Wolf, J. L. Zyskind, A. M. Vengsarkar, and J. Zhou, “A gain-flattened ultra wide band EDFA for high capacity WDM optical communications systems,” in *Proc. ECOC’98*, 1998, pp. 53–54.
- [6] M. Jinno, J. Sakamoto, J. Kani, S. Aisawa, K. Oda, M. Fukui, H. Ono, and K. Oguchi, “First demonstration of 1580 nm wavelength band WDM transmission for doubling usable bandwidth and suppressing FWM in DSF,” *Electron. Lett.*, vol. 33, no. 10, pp. 882–883, 1997.
- [7] M. Karasek, “Design of gain-shifted erbium-doped fiber amplifiers for WDM applications,” *IEE Proc.—Optoelectron.*, vol. 146, no. 3, pp. 143–148, 1999.
- [8] T. Sakamoto, K. Hittori, J. Kani, M. Fukutoku, M. Fukui, M. Jinno, and K. Oguchi, “Flat-gain operation of 1580 nm-band EDFA with gain variation of 0.2 dB over 1579–1592 nm,” *Electron. Lett.*, vol. 34, no. 20, pp. 1959–1960, 1998.
- [9] H. Ono, M. Yamada, M. Shimizu, and Y. Ohishi, “Single output characteristics of 1.58  $\mu\text{m}$  band gain flattened Er -doped fiber amplifiers for WDM systems,” *Electron. Lett.*, vol. 34, no. 15, pp. 1513–1514, 1998.

- [10] H. Ono, M. Yamada, M. Shimizu, and O. Ohishi, "Comparison of amplification characteristics of 1.58 and 1.55  $\mu\text{m}$  band EDFAs," *Electron. Lett.*, vol. 34, no. 15, pp. 1509–1510, 1998.
- [11] H. Ono, M. Yamada, T. Kanamori, and Y. Ohishi, "Low-noise and high-gain 1.58  $\mu\text{m}$  band Er -doped fiber amplifiers with cascade configurations," *Electron. Lett.*, vol. 33, no. 17, pp. 1477–1479, 1997.
- [12] R. M. Percival, S. Cole, D. M. Cooper, S. P. Craig-Ryan, A. D. Ellis, C. J. Rowe, and W. A. Stallard, "Erbium-doped fiber amplifier with constant gain for pump between 966 and 1004 nm," *Electron. Lett.*, vol. 27, no. 14, p. 1266, 1991.
- [13] B. Pedersen, B. A. Thompson, S. Zemon, W. J. Miniscalco, and T. Wei, "Power requirement for erbium-doped fiber amplifiers pumped in the 800, 980, and 1480 nm bands," *IEEE Photon. Technol. Lett.*, vol. 4, pp. 46–49, Jan. 1992.
- [14] F. A. Flood and C. C. Wang, "980-nm pump-band wavelengths for longwavelength-band erbium-doped fiber amplifier," *IEEE Photon. Technol. Lett.*, vol. 11, pp. 1232–1234, Oct. 1999.
- [15] J. F. Massicott, J. R. Armitage, R. Wyatt, B. J. Ainslie, and S. P. Craig-Ryan, "High gain, broadband, 1.6  $\mu\text{m}$  Er -doped silica fiber amplifier," *Electron. Lett.*, vol. 26, no. 20, pp. 1645–1646, 1990.
- [16] J. F. Massicott, R. Wyatt, and B. J. Ainslie, "Low noise operation of Er doped silica fiber amplifier around 1.6  $\mu\text{m}$ ," *Electron. Lett.*, vol. 28, no. 20, pp. 1924–1925, 1992.
- [17] R. Di Muro, N. E. Jolley, and J. Mun, "Measurement of the quantum efficiency of long wavelength EDFAs with and without an idler signal," in *Proc. ECOC'98*, 1998, pp. 419–420.
- [18] J. Lee, U.-C. Ryu, S. J. Ahn, and N. Park, "Enhancement of power conversion

- efficiency for an L-band EDFA with a secondary pumping effect in the unpumped EDF section,” *IEEE Photon. Technol. Lett.*, vol. 11, pp. 42–44, Jan. 1999.
- [19] J. Nilsson, S. Y. Yun, S. T. Hwang, J. M. Kim, and S. J. Kim, “Long wavelength erbium-doped fiber amplifier gain enhanced by ASE end reflectors,” *IEEE Photon. Technol. Lett.*, vol. 10, pp. 1551–1553, Nov. 1998.
- [20] K. J. Cordina, N. E. Jolley, and J. Mun, “Ultra low-noise long-wavelength EDFA with 3.6 dB external noise figure,” in *Proc. OFC’99*, paper WA5 1999.
- [21] H. Suzuki, M. Fujiwara, N. Takachio, K. Iwatsuki, T. Kitoh, and T. Shibata, “12.5-GHz spaced 1.28-Yb/s (512-channel  $\times$  2.5 Gb/s) super-dense WDM transmission over 320-km SMF using multiwavelength generation technique,” *IEEE Photon. Technol. Lett.*, vol. 14, pp. 405–407, 2002.
- [22] S. Yamashita, K. Hsu, and W.H. Loh, “Miniature erbium:ytterbium fiber Fabry-Perot multiwavelength lasers,” *IEEE J. Select Topics Quantum Electron.*, vol. 3, pp. 1058-1064, 1997.
- [23] A. J. Poustie, N. Finlayson, and P. Harper, “Multiwavelength fiber laser using a spatial mode beating fiber,” *Opt. Lett.*, vol.19, pp.716-718, 1994.
- [24] N. Park and P.F. Wysocki, “24-line multiwavelength operation of erbium-doped fiber-ring laser”, *IEEE Photon. Technol. Lett.*, vol. 8, pp. 1459–1461, 1996.
- [25] J. Chow, G. Town, B. Eggleton, M. Ibsen, K. Sugden, and I. Bennion, “Multiwavelength generation in an erbium-doped fiber laser using in-fiber comb filters,” *IEEE Photon. Technol. Lett.*, vol. 8, pp. 60–62, 1996.
- [26] S. Yamashita and K. Hotate, “Multiwavelength erbium-doped fiber laser using intra-cavity etalon and cooled by liquid nitrogen,” *Electron. Lett.*, vol. 32, pp. 1298-1299, 1996.
- [27] O. Graydon, W.H. Loh, R.I. Laming, and L. Dong, “Triple-frequency operation of



- an Er-doped twincore fiber loop laser,” *IEEE Photon. Technol. Lett.*, vol. 8, pp. 63–65, 1996.
- [28] A. Bellemare, M. Karasek, M. Rochette, S. LaRochelle, and M. Tutu, “Room temperature multifrequency erbium-doped fiber lasers anchored on the ITU frequency grid,” *J. Lightwave Technol.*, vol. 18, pp. 825-831, 2000.
- [29] G. J. Cowle and D.Y. Stepanov, “Multiple wavelength generation with Brillouin\_erbium fiber lasers,” *IEEE Photon. Technol. Lett.*, vol. 8, pp. 1465–1467, 1996.
- [30] M. Yamada, H. Ono, T. Kanamori, S. Sudo, and Y. Ohishi, “Broadband and gain-fallened amplifier composed of a 1.55  $\mu\text{m}$  band and a 1.58  $\mu\text{m}$ -band  $\text{Er}^{3+}$  doped silica fiber amplifier in a parallel configuration,” *Electron. Lett.*, vol. 33, pp.710-711, 1997.
- [31] A. Bellemare, M. Karasek, C. Riviere, F. Babin, G. He, V. Roy, and G. W. Schinn, “A broadly tunable erbium-doped fiber ring laser: Experimentation and modeling,” *IEEE J. Sel. Topics Quantum Electron.*, vol. 7, pp. 22–29, 2001.
- [32] X. Dong, N. Q. Ngo, P. Shum, H.-Y. Tam, and X. Dong, “Linear cavity erbium-doped fiber laser with over 100 nm tuning range,” *Opt. Exp.*, vol. 11, pp. 1689–1694, 2003.
- [33] X. Dong, H.-Y. Tam, B.-O. Guan, C.-L. Zhao, and X. Dong, “High power erbium-doped fiber ring laser with widely tunable range over 100 nm,” *Opt. Commun.*, vol. 224, no. 4–6, pp. 295–299, 2003.
- [34] C. C. Renaud, R. J. Selvas-Aguilar, J. Nilsson, P. W. Turner, A. B. Grudinin, “Compact High–Energy Q-Switched Cladding-Pumped Fiber Laser with a Tuning Range Over 40 nm,” *IEEE Photon. Technol. Lett.* vol. 11, pp.976-978, 1999.
- [35] S. Yamashita, and M. Nishihara, “Widely Tunable Erbium-Doped Fiber Ring

Laser Covering Both C-band and L-band,” *IEEE J. Sel. Top. Quantum Electron.*, vol. 7, pp.41-43, 2001.

- [36] M. Melo, O. Frazao, A. L. J. Teixeira, L. A. Gomes, J. R. Ferreira da rocha, and H. M. Salgado, “Tunable L-band erbium-doped fibre ring laser by means of induced cavity loss using a fibre taper,” *Appl. Phys. B*, vol. 77, pp.139-142, 2003.



## Chapter 2

# A power conversion efficiency improved L-band erbium-doped fiber amplifier

### 2.1 Introduction

The  $\text{Er}^{3+}$ -doped fiber amplifier (EDFA) with a flattened gain is a key device for wavelength division multiplexing (WDM) transmission systems and has been used in WDM transmission experiments at over 1 Tb/s [1]–[4]. An  $\text{Er}^{3+}$ -doped fiber has a 1580 nm amplification band in addition to the conventional 1550 nm amplification band. Using the 1580 nm amplification band has two advantages: The first is that it allows a conventional 1550 nm-band (C-band) EDFA to be combined with a 1580 nm-band (L-band) EDFA in a parallel configuration [5]–[7]. This realizes a broad amplification bandwidth EDFA that can expand the transmission capacity of WDM transmission systems [8]–[10]. The other is that by using the 1580 nm amplification band, we can construct an effective WDM system using dispersion-shifted fiber (DSF) to avoid the degradation caused by four-wave mixing (FWM) because the zero-dispersion wavelength of DSF is not in the 1580 nm band [11], [12].

The first study on 1580 nm band amplification reported that a 25 dB gain was obtained from 1570 to 1610 nm by using a silica-based  $\text{Er}^{3+}$ -doped fiber with a 1550 nm light as a pump [13], [14]. 1580 nm band amplification with 980 and 1480 nm band LD's and the investigation of WDM signal amplification characteristics are important if EDFA's are to be used in advanced systems [15]–[17]. 1580 nm band amplification by using an EDF with another glass as the  $\text{Er}^{3+}$  ion host [18] is interesting because it is expected that changing the host glass would yield different amplification characteristics.

An example is broadening and flattening the amplification band in the 1550 nm band by changing the host glass from silica-based glass to a fluoride glass [19, 20]

## 2.2 Experimental setup

Fig. 2.1 shows a L-band EDFA configuration used for the experiment. Because of ultra-wide amplified spontaneous emission spectrum [21] with comparable gain at a reduced fiber length and suppressed noise power, the high erbium ( $\text{Er}^{3+}$ ) concentration in a specially designed L-band fiber is adopted. The highly doped EDF is characterized by numerical aperture of 0.22, a cutoff wavelength of 954 nm, the attenuation of 5.9 dB/m at 1200 nm and the peak absorption of 11.7 dB/m at 980nm and 17 dB/m at 1531 nm. To generate optimal pumping scheme, the optional length of EDF used is 15 m, 30 m, 45 m, or 60 m. Besides, the EDF is forwardly pumped by a 980-nm or 1480-nm laser diode through a 980/1550-nm or 1480/1550 WDM fiber coupler and backwardly pumped by a 1480-nm laser diode through a 1480/1550-nm WDM fiber coupler. The wavelength of L-band signal from 1552 to 1590 nm is used for the experiments by tunable laser source. The power level used for the L-band signals is -20 dBm. Two optical isolators are used to ensure the unidirectional propagation of the light, thus preventing a spatial hole burning in the EDFA caused by bi-directional operation and simultaneously allowing a stable single-frequency operation.

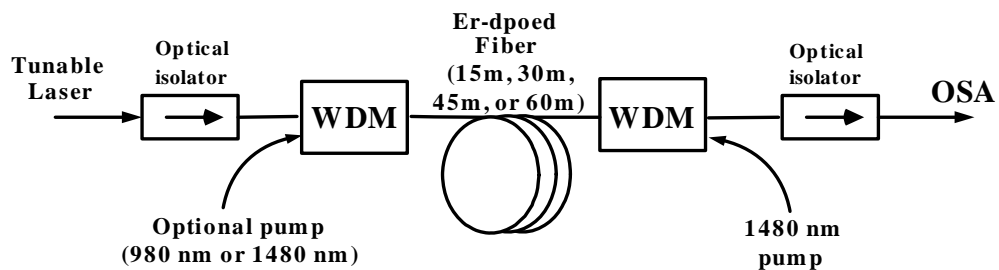


Fig. 2.1 The schematic diagram of the L-band EDFA.

## 2.3 Principle of 1580-nm Band Amplification

Fig. 2.2 shows the energy level diagram of  $\text{Er}^{3+}$  ion. 1580-nm band amplification, whose pump band is the 980- or 1480-nm is due to the  ${}^4\text{I}_{13/2} \rightarrow {}^4\text{I}_{15/2}$  stimulated emission [22], which is the same as 1550-nm band amplification, and is caused by the low energy transitions between the Stark components of the  ${}^4\text{I}_{13/2}$  and  ${}^4\text{I}_{15/2}$  manifolds.

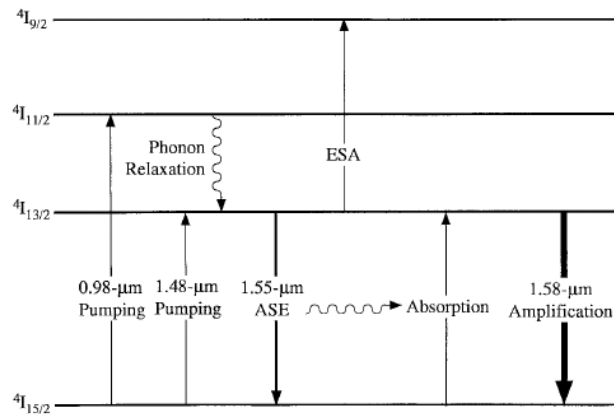


Fig. 2.2 Energy level diagram of the  $\text{Er}^{3+}$  ion. (After Ref. [22])

Fig. 2.3 shows a schematic diagram of 1580-nm band amplification. 1550-nm band amplified spontaneous emission (ASE) is generated by 980- or 1480-nm band pump light at the input portion of the fiber. The ASE is absorbed at the output portion, so 1580-nm band amplification is realized.

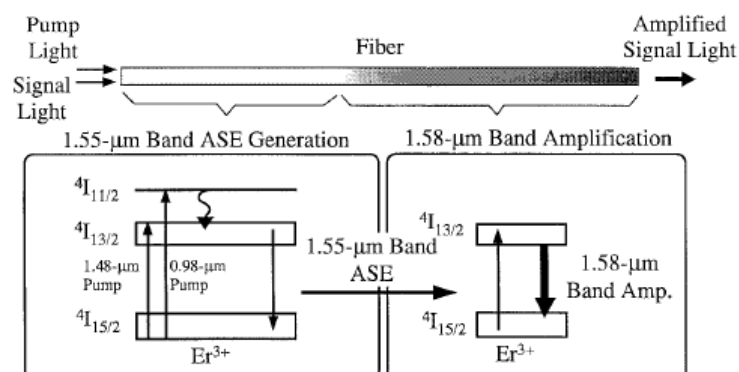


Fig. 2.3 Schematic diagram of 1580-nm band amplification. (After Ref. [22])

In general, the fiber length of  $\text{Er}^{3+}$ -doped fiber in L-band EDFA is longer than in C-band EDFA because the need of lower population inversion in L-band EDFA and the gain coefficient in the L-band is smaller than that in the C-band in lower population inversion situation, as shown in Fig. 2.4. The configuration of a 1580-nm band EDFA is the same as that of a 1550-nm band EDFA. Therefore, we can use the optical components used in the 1550-nm band EDFA such as the WDM coupler and isolator when constructing a 1580-nm band EDFA.

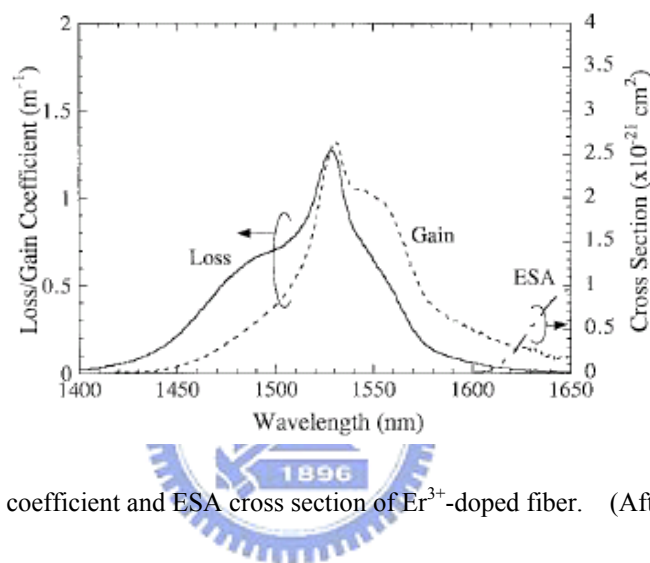


Fig. 2.4 Gain and loss coefficient and ESA cross section of  $\text{Er}^{3+}$ -doped fiber. (After Ref. [22])

## 2.4 Results and Discussion

### 2.4.1 Characteristics of optimized configuration

Several pumping schemes have been investigated in order to construct high-gain and high power conversion efficiency (PCE) L-band EDFA, as shown in Table 2.1.

Pumping Wavelength	Length (m)	PCE (%)	Gain(max) (dB)
980/1480	15	24.7	30.9
1480/1480	15	21.2	35.7
980/1480	30	36.55	33.5
1480/1480	30	33.08	37.2
980/1480	45	30.6	31.1
1480/1480	45	37	34.8
980/1480	60	20	35.2
1480/1480	60	23.6	38.5

Table 2.1 Power conversion efficiency (PCE) and the maximum gain of the EDFA pumped at different forward/backward schemes.

Each pumping scheme of the measured results is optimized by adjusting the length of EDF and pumping power (forward and backward). Because of economic benefits, the fiber length of 30 m and a 980nm (forward)/1480nm (backward) cascaded pumping geometry is selected. The forward pumping at 980nm is effective for improving the noise characteristics, while the backward pumping at 1480nm benefits from a better quantum conversion efficiency and gain coefficient [23]. With such a simplified EDFA, an extremely high power conversion efficiency (PCE) of 37% is achieved. The high PCE shows more than 10% improvement as compared to that reported using conventional L-band EDFA configuration [24]. The PCE is giving by the following equation:

$$PCE = \frac{(P_{sigout} - P_{sign})}{P_{pump}} \quad (2.4.1-1)$$

where  $P_{sigout}$ ,  $P_{sign}$ , and  $P_{pump}$  denote the signal output power, signal input power, and pump power, respectively. Simply speaking, the PCE is the amplification of input signal power resulted from every unit pumping power.

Fig. 2.5 shows the typical output ASE spectrum of the optimized L-band EDFA ranged between 1525 nm and 1612 nm. From the shape of the spectrum, the gain coefficient in L-band is clearly larger than theoretical value due to the specially designed L-band

EDF.

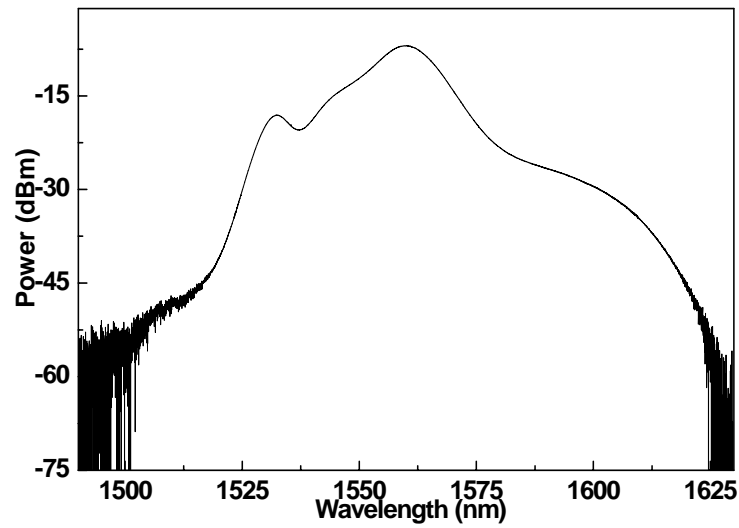


Fig. 2.5 Output ASE spectrum of the L-band EDFA

Fig. 2.6 shows the small-signal gain profile of the L-band EDFA from 1552 nm to 1590 nm at input signal power of -20 dBm. The wavelength dependent gain deviation of 6 dB in L-band is obtained.

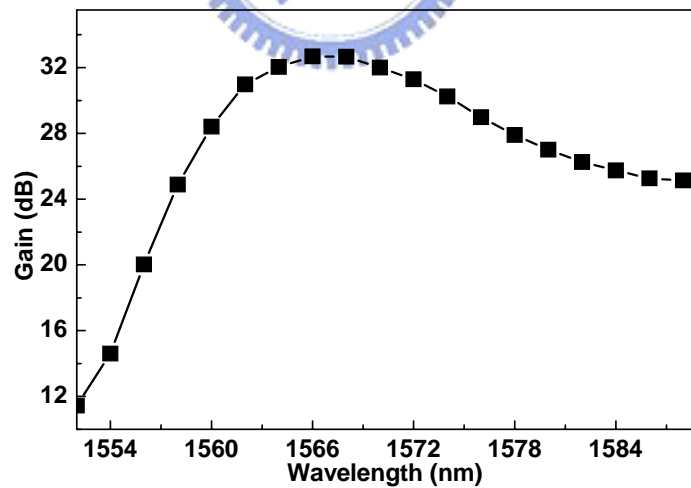


Fig. 2.6 Small-signal gain of the EDFA at input signal power of -20 dBm.

## 2.5 Conclusions

We have demonstrated the use of highly  $\text{Er}^{3+}$ -doped silica fiber as a L-band amplifier, obtaining in excess of 24.5 dB of small signal gain between 1560 nm and 1590 nm by



forward pumping at 980 nm with power of 17.5 mW and backward pumping at 1480 nm with power of 200mW when the EDF length is 30 m. With such a simplified EDFA, an extremely high power conversion efficiency (PCE) of 37% with a wavelength dependent gain deviation of 6 dB is achieved. The high PCE shows more than 10% improvement as compared to that reported using conventional L-band EDFA configuration.

## 2.6 References

- [1] H. Onaka, H. Miyata, G. Ishikawa, K. Otsuka, H. Ooi, Y. Kai, S. Kinoshita, M. Seino, H. Nishimoto, and T. Chikama, "1.1 Tb/s WDM transmission over a 150 km 1.3  $\mu\text{m}$  zero-dispersion single-mode fiber," in *Proc. OFC'96*, 1996, postdeadline papers, PD19.
- [2] A. H. Gnauck, A. R. Chraplyvy, R. W. Tkach, J. L. Zyskind, J. W. Sulhoff, A. J. Lucero, Y. Sun, R. M. Jopson, F. Forghieri, R. M. Derosier, C. Wolf, and A. R. McCormick, "One terabit/s transmission experiment," in *Proc. OFC'96*, 1996, postdeadline papers, PD20.
- [3] T. Morioka, H. Takara, S. Kawanishi, O. Kamatani, T. Takiguchi, K. Uchiyama, M. Saruwatari, H. Takahashi, M. Yamada, T. Kanamori, and H. Ono, "100 Gbit/s  $\times$  10 channel OTDM/WDM transmission using a single-mode supercontinuum WDM source," in *Proc. OFC'96*, 1996, postdeadline papers, PD21.
- [4] Y. Yano, T. Ono, K. Fukuchi, T. Ito, H. Yamazaki, M. Yamaguchi, and K. Emura, "2.6 Terabit/s WDM transmission experiment using optical duobinary coding," in *Proc. ECOC'96*, 1996, post-deadline papaers, ThB3.1.
- [5] M. Yamada, H. Ono, T. Kanamori, S. Sudo, and Y. Ohishi, "Broadband and gain-flattened amplifier composed of a 1.55  $\mu\text{m}$ -band and a 1.58  $\mu\text{m}$ -band

- Er<sup>3+</sup>-doped fiber amplifier in a parallel configuration,” *Electron. Lett.*, vol. 33, pp. 710–711, 1997.
- [6] Y. Sun, J. W. Sulhoff, A. K. Srivastava, J. L. Zyskind, T. A. Strasser, J. R. Pedrazzani, C. Wolf, J. Zhou, J. B. Judkins, R. P. Espindola, and A. M. Vengsarkar, “80 nm ultra-wideband erbium-doped silica fiber amplifier,” *Electron. Lett.*, vol. 33, pp. 1965–1967, 1997.
- [7] K. Suzuki, H. Masuda, S. Kawai, K. Aida, and K. Nakagawa, “Bidirectional 10-channel 2.5 Gbit/s WDM transmission over 250 km using 76 nm (1531–1607 nm) gain-band bidirectional erbium-doped fiber amplifier,” *Electron. Lett.*, vol. 33, no. 23, pp. 1967–1968, 1997.
- [8] T. Sakamoto, J. Kani, M. Jinno, S. Aisawa, M. Fukui, M. Yamada, and K. Oguchi, “Wide wavelength band (1535–1560 nm and 1574–1600 nm), 28 × 10 Gbit/s WDM transmission over 320 km dispersion-shifted fiber,” *Electron. Lett.*, vol. 34, no. 4, pp. 392–394, 1998.
- [9] A. K. Srivastava, Y. Sun, J. W. Sulhoff, C. Wolf, M. Zringibl, R. Monnard, A. R. Chraplyvy, A. A. Abramov, R. P. Espindola, T. A. Strasser, J. R. Pedrazzani, A. M. Vengsarkar, J. L. Zyskind, J. Zhou, D. A. Ferrand, P. F. Wysocki, J. B. Judkins, and Y. P. Li, “1 Tb/s transmission of 100 WDM 10 Gb/s channels over 400 km of truewave fiber,” in *Proc. OFC’98*, 1998, postdeadline papers, PD10.
- [10] S. Aisawa, T. Sakamoto, M. Fukui, J. Kani, M. Jinno, and K. Oguchi, “Ultra-wideband, long distance WDM demonstration of 1 Tbit/s (50 × 20 Gbit/s), 600 km transmission using 1550 and 1580 nm wavelength bands,” *Electron. Lett.*, vol. 34, no. pp. 1127–1129, 1998.
- [11] M. Jinno, T. Sakamoto, J. Kani, S. Aisawa, K. Oda, M. Fukui, H. Ono, and K. Oguchi, “First demonstration of 1580 nm wavelength band WDM transmission,”

in *Proc. OECC'97*, Tech. Dig., Seoul, Korea, 1997, pp. 406–407.

- [12] T. Sakamoto, M. Fukui, M. Jinno, J. Kani, S. Aisawa, H. Ono, M. Yamada, and K. Oguchi, “Recirculating loop experiment for 1580-nm band large-scale WDM network using dispersion-shifted fiber,” *IEEE Photon. Technol. Lett.*, vol. 10, pp. 618–620, Apr. 1998.
- [13] J. F. Massicott, J. R. Armitage, R. Wyatt, B. J. Ainslie, and S. P. Craig-Ryan, “High gain, broadband, 1.6  $\mu\text{m}$   $\text{Er}^{3+}$  doped silica fiber amplifier,” *Electron. Lett.*, vol. 26, no. 20, pp. 1645–1646, 1990.
- [14] J. F. Massicott, R. Wyatt, and B. J. Ainslie, “Low noise operation of  $\text{Er}^{3+}$  doped silica fiber amplifier around 1.6  $\mu\text{m}$ ,” *Electron. Lett.*, vol. 28, no. 20, pp. 1924–1925, 1992.
- [15] H. Ono, M. Yamada, and Y. Ohishi, “Gain-flattened  $\text{Er}^{3+}$ -doped fiber amplifier for a WDM signal in the 1.57–1.60- $\mu\text{m}$  wavelength region,” *IEEE Photon. Technol. Lett.*, vol. 9, pp. 596–598, May 1997.
- [16] H. Ono, M. Yamada, S. Sudo, and Y. Ohishi, “1.58  $\mu\text{m}$  band  $\text{Er}^{3+}$ -doped fiber amplifier pumped in the 0.98 and 1.48  $\mu\text{m}$  bands,” *Electron. Lett.*, vol. 33, no. 10, pp. 876–877, 1997.
- [17] Y. Sun, W. Shulhoff, A. K. Srivastava, J. L. Zyskind, and C. Wolf, “An 80 nm ultra wide band EDFA with low noise figure and high output power,” in *Proc. ECOC'97, Edinburgh, UK*, 1997, vol. 5, pp. 69–72, postdeadline papers.
- [18] H. Ono, M. Yamada, T. Kanamori, S. Sudo, and Y. Ohishi, “1.58  $\mu\text{m}$  band fluoride-based  $\text{Er}^{3+}$ -doped fiber amplifier for WDM transmission systems,” *Electron. Lett.*, vol. 33, no. 17, pp. 1471–1472, 1997.
- [19] B. Clesca, D. Ronarc'h, D. Bayart, Y. Sorel, L. Hamon, M. Guibert, L. Beylat, J. F. Kerdiles, and M. Semenkoff, “Gain flatness comparison between erbium-doped

- fluoride and silica fiber amplifiers with wavelength-multiplexed signals,” *IEEE Photon. Technol. Lett.*, vol. 6, pp. 509–512, Apr. 1994.
- [20] M. Yamada, T. Kanamori, Y. Terunuma, K. Oikawa, M. Simizu, S. Sudo, and K. Sagawa, “Fluoride-based erbium-doped fiber amplifier with inherently flat gain spectrum,” *IEEE Photon. Technol. Lett.*, vol. 8, pp. 882–884, July 1996.
- [21] M. Melo, A. Teixeira, L.A. Gomes, C. Santos, D. Pereira, O. Fraz ao, P. Andr’e, M. Lima, F. Rocha, H.M. Salgado: *In: Proc. Portuguese Conf. F’isica 2002*, pp. 556–557
- [22] H. Ono, M. Yamada, T. Kanamori, S. Sudo, and Y. Ohishi, ”1.58- $\mu$ m Band Gain-Flattened Erbium-Doped Fiber Amplifiers for WDM Transmission Systems,” *Journal of Lightwave Techno.*, vol. 17, pp.490–496, 1999.
- [23] X. Y. Dong, P. Shum, N. Q. Ngo, H. Y. Tam, X. Y. Dong, “Output Power Characteristics of Tunable Erbium-Doped Fiber Ring Lasers,” *J. Lightwave Technol.*, vol. 23, pp. 1334-1341, 2005.
- [24] J. Lee, U. C. Ryu, S. J. Ahn, and N. Park, “Enhancement of Power Conversion Efficiency for an L-band EDFA with a Secondary Pumping Effect in the Unpumped EDF Section,” *IEEE Photon. Technol. Lett.*, vol. 11, pp. 42-44, 1999.

# Chapter 3

## A coupler and air-gap etalon controlled high-efficiency L-band erbium-doped fiber laser

### 3.1 Introduction

Owing to the insufficient channel capacity of the current dense wavelength division multiplexed (DWDM) systems, long-wavelength band erbium-doped fiber amplifier (EDFA) with wavelength ranging from 1570 nm to 1610 nm [1] have been investigated in order to widen the transmission capacity. In addition, L-band tunable fiber lasers are essential for testing the L-band devices used in WDM transmission systems. Therefore, the realization of economical and efficient L-band fiber laser architecture becomes necessary for its commercialization. Previously, the gain medium for L-band fiber laser includes dense erbium-doped fiber, erbium-ytterbium co-doped double clad fiber [2], and brillouin-erbium fiber [3], etc. Typically, the L-band erbium-doped fiber laser (EDFL) can be configured with such as dual resonant cavity [4], linear overlapping cavity [5], and single ring cavity [6]. The wavelength-tuning are mainly based on the intra-cavity Fabry–Perot filters [7], fiber Bragg gratings (FBGs) [8], and cavity loss [9] adjustment. In particular, the wavelength tunability of L-band EDFL via cavity loss control was simply demonstrated by optomechanically bending the single-mode fiber in the EDFL cavity [9]. To meet the cost-effective demand, we present a coupling-ratio controlled wavelength-tuning, full L-band erbium-doped fiber ring laser (EDFRL) with a tunable range over 45nm and low variation ( $<1.2\text{dB}$ ) of the output laser power over all the tuning range. In addition, the quantum efficiency of the EDFRL which

simultaneously reaches an extremely high value is 42%. In the aspect of EDFA, by using highly doped EDF and adjusting fiber length, an optimized bi-directional pumped L-band EDFA of the EDFL which possesses extremely high power conversion efficiency (PCE) about 37% provides gain to the loop. The high PCE shows more than 10% improvement compared with that reported using conventional L-band EDFA [10] configuration.

### 3.2 Theory of wavelength shifting phenomenon

The theoretical model is based on the scheme depicted in Fig. 3.1 [11]. The active medium is an  $\text{Er}^{3+}$ -doped fiber amplifier (EDFA) of length  $L$  described by the three-level system rate equations [12]:

$$\frac{dP_p(z)}{dz} = -\sigma_p A_p \rho n_1 P_p(z), \quad (1)$$

$$\frac{dP_s(z)}{dz} = A_s \rho [\sigma_E(\lambda) n_2 - \sigma_A(\lambda) n_1] P_s(z), \quad (2)$$

$$n_2 = \left\{ n_1 \frac{P_p(z)}{P_{p\text{sat}}} - \left[ n_2 - \frac{\sigma_A(\lambda)}{\sigma_E(\lambda)} n_1 \right] \frac{P_s(z)}{P_{s\text{sat}}} \right\}, \quad (3)$$

$$n_1 = 1 - n_2, \quad (3)$$

where

$$P_{p\text{sat}} = \frac{h\nu_p A}{\sigma_p \tau A_p}, \quad P_{s\text{sat}} = \frac{h\nu_s A}{\sigma_E \tau A_s}. \quad (4)$$

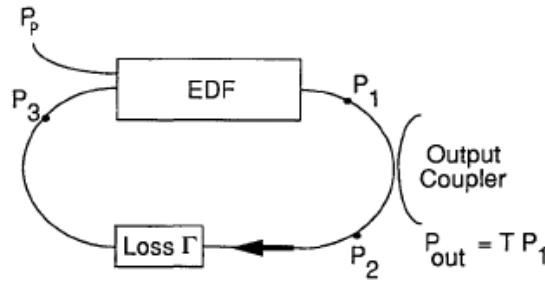


Fig. 3.1 Scheme of the unidirectional EDFL (after Ref. [12])

The quantities appearing in the above formulas are defined as follows:  $P_p(z)$  is the pump

power at the longitudinal coordinate  $z$  inside the active fiber,  $P_s(z)$  the forward signal power,  $\sigma_p$  the pump absorption cross section,  $\sigma_{E,A}(\lambda)$  the emission and the absorption cross sections,  $\rho$  the dopant concentration,  $A_{p,s}$  the pump and the signal overlap integrals,  $n_{1,2}$  the lower and the upper laser level population fractions,  $\tau$  the upper laser level lifetime, and  $A$  the fiber core area. Because the laser operates unidirectionally, the backward signal power has been neglected.

The laser cavity has a loss (see Fig. 3.1)

$$\Gamma_{TOT} \equiv P_1 / P_3, \quad (5)$$

which can be conveniently attributed to two different contributions.

The first contribution is the output coupler loss  $\gamma$ . If the coupler extracts a fraction  $T$  of the power, we have

$$P_{out} = TP_1, \quad 0 < T < 1, \quad (6)$$

and hence

$$\gamma \equiv \frac{P_1}{P_2} = \frac{1}{1-T}, \quad \gamma > 1. \quad (7)$$



The second loss contribution comes from the intrinsic cavity loss defined as

$$\Gamma \equiv P_2 / P_3, \quad \Gamma > 1, \quad (8)$$

so that the total cavity loss  $\Gamma_{TOT}$  can be expressed as

$$\Gamma_{TOT} \equiv P_1 / P_3 = \gamma\Gamma. \quad (9)$$

As is well known [13], for laser emission to occur it is necessary that the amplifier gain  $G$  satisfy the threshold condition

$$G(\lambda_0) = \Gamma_{TOT}(\lambda_0), \quad G(\lambda \neq \lambda_0) < \Gamma_{TOT}(\lambda), \quad (10)$$

where  $\lambda_0$  is the emission wavelength. Note that including a wavelength dependence in  $\Gamma_{TOT}$  also accounts for any cavity element that may spectrally modulate the transmission (etalons, Lyot filters, etc.).

In the case of an EDFA the gain is [14]

$$G(\lambda, L) = \exp\{A_s \rho \int_0^L [\sigma_E(\lambda)n_2 - \sigma_A(\lambda)n_1] dz\}, \quad (11)$$

and hence, from Eq. (1) and the second of Eq. (3),

$$G(\lambda, L) = \exp\left\{g(\lambda)L + \frac{g(\lambda) + a(\lambda)}{\alpha_p} \ln\left[\frac{P_p(L)}{P_p(0)}\right]\right\}, \quad (12)$$

where  $g(\lambda) = \sigma_E A_s \rho$ ,  $a(\lambda) = \sigma_A(\lambda) A_s \rho$ , and  $\alpha_p = \sigma_p A_p \rho$  are the gain, the attenuation,

and the pump absorption coefficients, respectively. Introducing conditions (10), we

find that the laser operates at the wavelength that satisfies the following relation:

$$\max_{\lambda} \left\{ g(\lambda)L + \frac{g(\lambda) + a(\lambda)}{\alpha_p} \ln\left[\frac{P_p(L)}{P_p(0)}\right] - \ln[\Gamma_{TOT}(\lambda)] \right\} = 0. \quad (13)$$

Equivalently, the minimization with respect to  $\lambda$  of

$$\ln\left[\frac{P_p(L)}{P_p(0)}\right] = -\alpha_p \frac{g(\lambda)L - \ln[\Gamma_{TOT}(\lambda)]}{g(\lambda) + a(\lambda)} \equiv -\alpha_p \Psi(\lambda), \quad (14)$$

determines the emission wavelength of the laser.

Note that when the cold-cavity loss  $\Gamma_{TOT}$  is changed the emission wavelength  $\lambda$  changes, too. Because the derivative of Eq. (14) is an implicit expression containing the dependence of the emission wavelength on cavity loss, gain, and the attenuation coefficient, the minimum of Eq. (14) can be found numerically.

### 3.3 Experimental Setup

The experimental setup of the coupling-ratio controlled wavelength-tunable EDFL is shown in Fig. 3.2. It consists of an optimized L-band EDFA with a bi-directionally 980/1480 pumping scheme. According to chapter 2, the optimized operation, a 17.5mW forward pumping at 980 nm and a 200mW backward pumping at 1480 nm is employed.



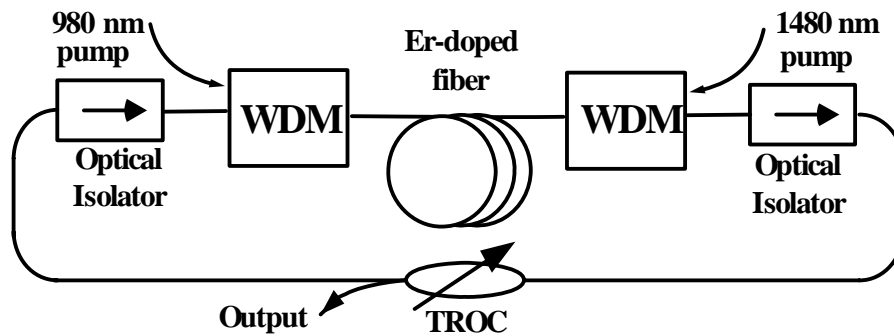


Fig. 3.2 The schematic diagram of the L-band EDFA. A coupling-ratio controlled wavelength tunable L-band EDFA with a tunable-ratio optical coupler (TROC).

This EDFA further takes the advantage of high erbium ( $\text{Er}^{3+}$ ) concentration in a specially designed L-band fiber, which offers an ultra-wide amplified spontaneous emission spectrum ranged between 1525 nm and 1612 nm (see Fig. 2.5) with comparable gain (see Fig. 2.6) at a reduced fiber length and suppressed noise power. The forward and backward pumping powers are launched into the EDF by a 980nm/1550nm and a 1480nm/1550nm WDM couplers, respectively. Two optical isolators are used to ensure the unidirectional propagation of the light, thus preventing spatial hole burning in the EDFA caused by bi-directional operation and simultaneously allowing a stable single-frequency operation. In particular, a  $1 \times 2$  tunable-ratio optical coupler (TROC) with variable output coupling ratio is inserted into the close-loop EDFA ring-cavity. The coupling ratio can be manually detuned from 0.5% to 99.5%. Initially, the output coupling ratio is set at 90% to obtain maximum output power.

### 3.4 Results and discussions

Several pumping schemes have been investigated in order to construct low-noise and high-gain L-band EDFA as the gain medium, and a 980nm (forward)/1480nm (backward) cascaded pumping geometry is selected. The forward pumping at 980nm

is effective for improving the noise characteristics, while the backward pumping at 1480nm benefits from a better quantum conversion efficiency and gain coefficient [15]. With such a simplified EDFA, an extremely high PCE of 37% with a wavelength dependent gain deviation of 6 dB is achieved according to chapter 2.

Figure 3.3 illustrates the output laser wavelength, power, and corresponding quantum efficiency as a function of the output coupling ratio detuned by the TROC. As a result, the wavelength of the EDFL with maximum output power can be linearly tunable from 1567 nm to 1612 nm as the output coupling ratio of the TROC detunes from 95% to 5%, while the output power of the EDFL is monotonically decreasing from 90 mW to 7 mW, as shown in Fig. 3.3.

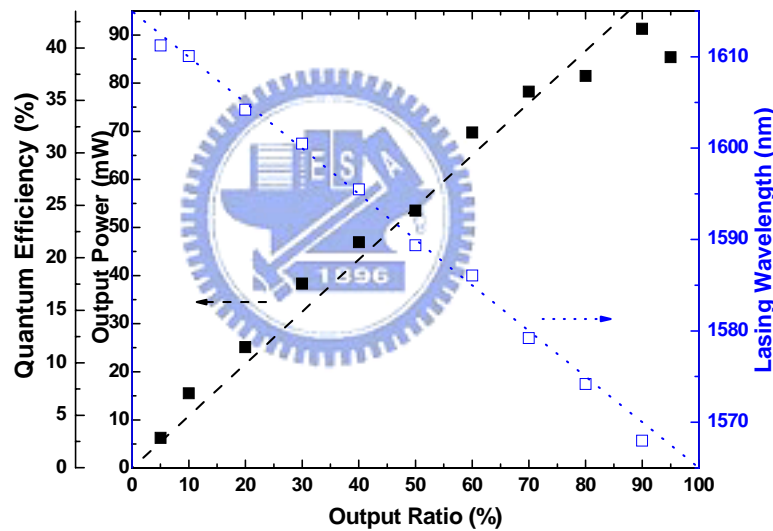


Fig. 3.3 The trend of lasing wavelength, output power, and quantum efficiency with detuning output coupling ratio.

It is seen that higher output coupling ratios as well as intra-cavity losses result in the EDFL lasing at shorter wavelengths. The lasing spectra of the EDFL at wavelengths corresponding to maximum output power also corroborates the maximum tuning range up to 45 nm (see Fig. 3.4).

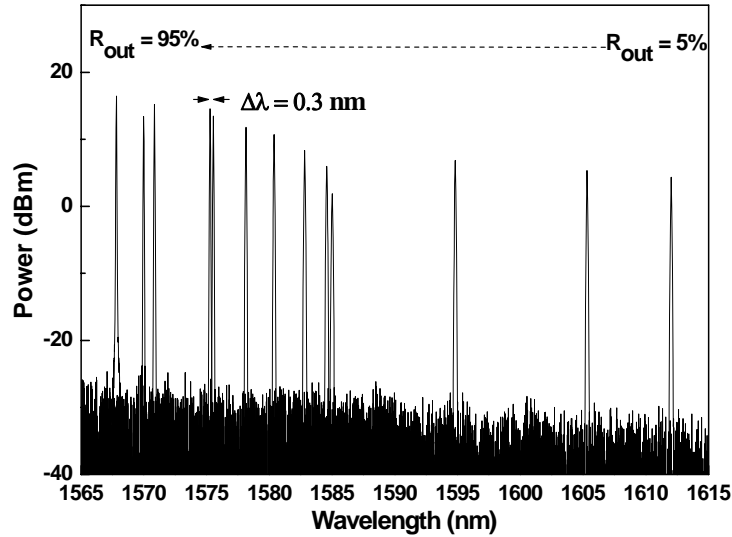


Fig.3.4 The lasing spectra of L-band EDFL with detuning output coupling ratio.

Previously, a similar simulating result concerning with the cavity-loss dependent tuning range of L-band EDFL system was proposed, which described a increasing sensitivity of the EDFL output power and bandwidth at lower intra-cavity losses. As the cavity-loss increases, the maximum output power and the wavelength tuning range are concurrently reduced [16]. By using the TROC based coupling ratio detuning technique, our experimental results not only correlate well with the theoretical observation, but also demonstrate the coupling-ratio dependent peak EDFL wavelength shifting phenomenon. These results sophisticate the operation of a widely tunable L-band EDFL since the minimizing in intra-cavity loss may achieve an extremely large tuning range at a scarification on output power of the EDFL, as shown in Fig. 3.4. Nonetheless, an accurate and repeatable wavelength selection is easily achieved with precise control on the output coupling ratio. In experiment, a minimum wavelength tuning resolution of 0.3 nm can be obtained under a change in coupling ratio of 0.6%, corresponding to tuning slope of 0.5 nm/%. On the other hand, the theoretical simulation also interpreted that the maximum tuning range of the L-band EDFL is greatly reduced when increasing output coupling ratio from 0.1 to 0.99. A maximum

and stable output power associated with a maximum quantum efficiency of up to 42% is obtained at an output coupling ratio of 0.9, as shown in Fig. 3.3. Even at a low-output and wide-band tunable condition with coupling ratio of only 10 %, the corresponding quantum efficiency of 8% can be still comparable with previous results [16, 17].

Each output channel exhibits the power of greater than 18.4 dBm and the maximum of 19.6 dBm at output coupling ratio of 90% is observed under the pumping power of 217.5 mW, as shown in Fig. 3.5. Such a deviation of 1.2 dB is already smaller than the best value of 1.5 dB in previous reports [9]. Moreover, a highly stable output with power variation of 0.036mW (0.04%) is obtained during a monitoring interval over 10 min, as shown in the right inset of Fig. 3.6.

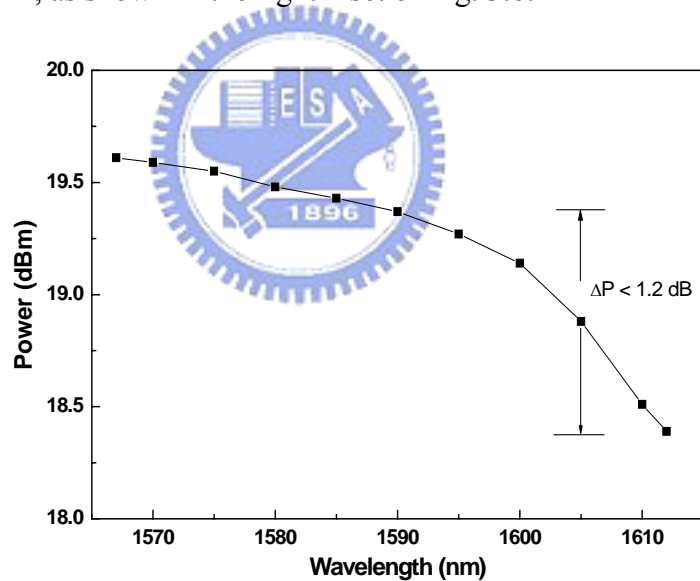


Fig. 3.5 Wavelength dependent output power at 90% output coupling ratio.

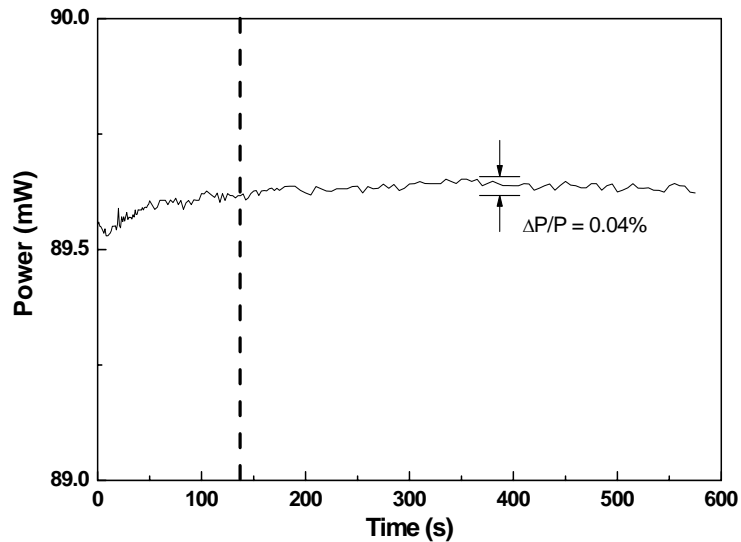


Fig. 3.6 Power stability of the L-band EDFL measured within 10 minutes.

The tuning range and resolution of lasing wavelength was mainly determined by the gain profile of the EDF since dynamic range on the coupling ratio of the TROC is nearly 100% in our case. The EDFL is unable to operate in the C-band with insufficient gain as the design of the specific EDF which benefits from a better transition of the power from C-band to L-band. Note that the lasing linewidth of the EDFL output can be further narrowing from 0.05 nm to 0.02 nm by simply inserting a tiny air-gap between the FC/PC connectors of fiber patch cord, which functions as an intra-cavity Fabry-Perot filter in the cost-effective L-band EDFL system, as shown in Fig. 3.7. The measured linewidth maybe somewhat limited by the commercial optical spectrum analyzer (Ando AQ6317B). Figure 3.8 shows the variation of 3-dB spectral linewidth when the spacing of air-gap is detuned, and the inset is the scheme of air-gap. Such a system benefits from not only the simplified wavelength tuning technique but also the cost-effective solution to the full L-band fiber laser systems.

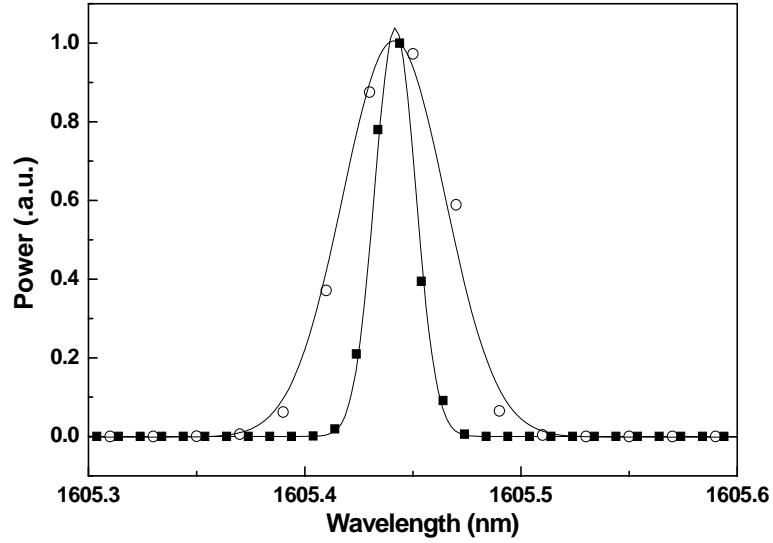


Fig. 3.7 The lasing linewidth without (hollow circle) or with (solid square) an air-gap inserting between FC/PC fiber connectors.

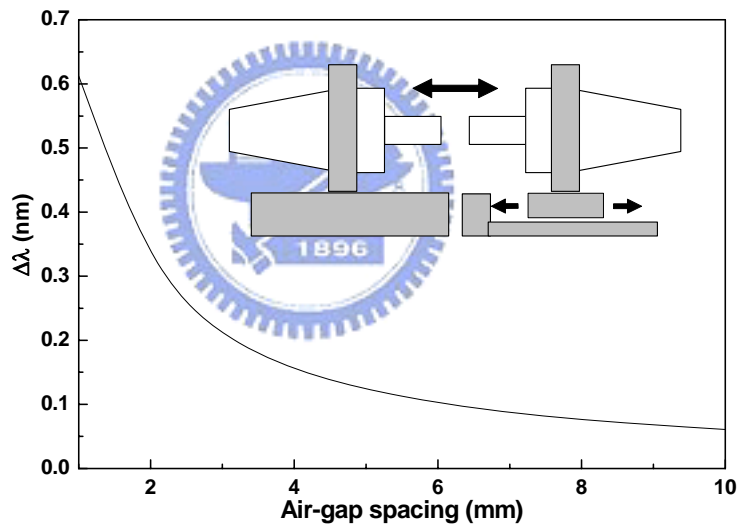


Fig 3.8 The variation of the 3-dB spectral linewidth when the spacing of air-gap is detuned.

### 3.5 Conclusions

We have experimentally investigated and demonstrated an output-coupling-ratio controlled, full long-wavelength-band erbium-doped fiber ring laser by using a bi-directionally dual-wavelength pumped EDFA in close-loop with a tunable ratio optical coupler. The L-band EDFL is wavelength-tunable from 1567 nm to 1612 nm

at a maximum quantum efficiency of 42%, respectively with ultra-high power conversion efficiency of 37%, comparable gain of 34 dB, and maximum output power of up to 91mW. The minimum wavelength tuning resolution of 0.3 nm is achieved under the maximum wavelength tuning range of up to 45 nm covering whole L-band, while a low channel power variation of <1.2dB and a stable output with 0.04% power fluctuation is observed.

### 3.6. APPENDIX A

In this appendix we show the derivation of Eq. (14) from Eq. (13). Let us consider two positive functions  $y(\lambda)$  and  $w(\lambda)$  and let us suppose that we intend to solve

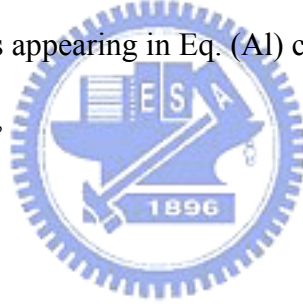
$$\max_{\lambda} [y(\lambda) + Aw(\lambda)] = 0. \quad (\text{A1})$$

From Eq. (13), the quantities appearing in Eq. (A1) can be identified as

$$y(\lambda) = g(\lambda)L - \ln[\Gamma_{TOT}(\lambda)],$$

$$w(\lambda) = \frac{g(\lambda) + a(\lambda)}{\alpha_p},$$

$$A = \ln \left[ \frac{P_p(L)}{P_p(0)} \right].$$



Since the laser can operate only if the gain at complete inversion  $\exp[g(\lambda)L]$  is greater than the cavity loss  $\Gamma_{TOT}(\lambda)$ , then  $y(\lambda)$  is a positive function.

Condition (A1) is equivalent to the following set of relations:

$$y(\lambda) + Aw(\lambda) = 0, \quad (\text{A2})$$

$$y'(\lambda) + Aw'(\lambda) = 0, \quad (\text{A3})$$

$$y''(\lambda) + Aw''(\lambda) < 0, \quad (\text{A4})$$

where the primes indicate derivation with respect to  $\lambda$ .

Equation (A2) indicates that, for a given wavelength  $\lambda$ , the laser reaches the oscillation threshold. In fact, with  $y(\lambda) + Aw(\lambda)$  being the net gain coefficient, Eq.

(A2) has to be null. Equation (A3) and inequality (A4) serve to yield the wavelength  $\lambda$  that maximizes the gain.

From Eq. (A2) we get  $A = -y(\lambda)/w(\lambda)$  and hence, by making use of Eq. (A3),

$$y'(\lambda)w(\lambda) - y(\lambda)w'(\lambda) = 0, \quad (\text{A5})$$

i.e.,

$$\frac{d}{d\lambda} \left[ \frac{y(\lambda)}{w(\lambda)} \right] = 0. \quad (\text{A6})$$


Moreover, we have

$$\frac{d^2}{d\lambda^2} \left[ \frac{y(\lambda)}{w(\lambda)} \right] = \frac{y''(\lambda) + Aw''(\lambda)}{w(\lambda)} < 0, \quad (\text{A7})$$

where we used relations (A2), (A4), and (A5).

This result proves that we can find the maximum in Eq. (A1), i.e., in Eq. (13), by maximizing  $y(\lambda)/w(\lambda)$ , or, equivalently, by minimizing  $A = -y(\lambda)/w(\lambda)$  as in Eq. (14).

### 3.7 References

- 
- [1] Y. Sun, J. W. Shlhoff, A. K. Srivastava, J. L. Zyskind, T. A. Strasser, J. R. Pedrazzani, C. Wolf, J. Zhou, J. B. Judkins, R. P. Espindola, and A. M. Vengasarkar, "80nm ultra-wideband erbium-doped silica fibre amplifier," *Electron. Lett.*, vol. 33, 1965-1967 (1997).
- [2] S. M. Zhang, Y. F. Lu, X. F. Yang, F. J. Dong, H. J. Wang, and X. Dong, "Wavelength tunable linear cavity cladding pump Er<sup>3+</sup>/Yb<sup>3+</sup> co-doped fiber laser operating in L-band," *Opt. and Quantum Electron.*, vol. 37, 417-424 (2005).
- [3] T. A. Haddud, M. H. Al-Mansoori, A. K. Zamzuri, S. Shaharudin, M. K. Abdullah, and M. A. Mahdi, "24-Line of Brillouin-Erbium Fiber Laser Utilizing Fabry-Perot Cavity in L-band," *Microwave Opt. Techno. Lett.*, vol. 45, 165-167 (2005).



- [4] S. W. Harun, and H. Ahmad, "Multiwavelength Laser Comb in L-band Region with Dual-Cavity Brillouin/Erbium Fiber Laser," *Jpn. J. Appl. Phys.*, vol. 41, L1234-L1236 (2002).
- [5] Q. H. Mao, and W. Y. Lit, "Optical Bistability in an L-Band Dual-Wavelength Erbium-Doped Fiber Laser with Overlapping cavities," *IEEE Photon. Technol. Lett.*, vol. 14, 1252-1254 (2002).
- [6] H. Chen, M. Leblanc, G. W. Schinn, "Gain enhanced L-band optical fiber amplifiers and tunable fiber lasers with erbium-doped fibers," *Opt. Commun.*, vol. 216, 119-125 (2003).
- [7] Q. H. Mao, and W. Y. Lit, "Widely tunable L-band erbium-doped fiber laser with fiber Bragg gratings based on optical bistability," *App. Phys. Lett.*, vol. 82, 1335-1337 (2003).
- [8] X. H. Feng, Y. G. Liu, S. H. Yuan, G. Y. Kai, W. G. Zhang, and X. Y. Dong, "L-Band switchable dual-wavelength erbium-doped fiber laser based on a multimode fiber Bragg grating," *Opt. Express*, vol. 12, 3834-3839 (2004).
- [9] M. Melo, O. Frazao, A. L. J. Teixeira, L. A. Gomes, J. R. Ferreira da rocha, and H. M. Salgado, "Tunable L-band erbium-doped fibre ring laser by means of induced cavity loss using a fibre taper," *Appl. Phys. B*, vol. 77, 139-142 (2003).
- [10] J. Lee, U. C. Ryu, S. J. Ahn, and N. Park, "Enhancement of Power Conversion Efficiency for an L-band EDFA with a Secondary Pumping Effect in the Unpumped EDF Section," *IEEE Photon. Technol. Lett.*, vol. 11, 42-44 (1999).
- [11] P. Franco, M. Midrio, and A. Tozzato, "Characterization and optimization criteria for filterless erbium-doped fiber lasers," *J. Opt. Soc. Am. B*, vol.11, 1090-1097 (1994).

- [12] E. Desurvire and J. R. Simpson, "Amplification of spontaneous emission in erbium-doped single-mode fibers," *IEEE J. Lightwave Technol.*, vol. 7, 835 (1989).
- [13] A. E. Siegman, "An Introduction to Lasers and Masers(McGraw-Hill, New York, 1971)".
- [14] C. R. Giles and D. DiGiovanni, "Spectral dependence of gain and noise in erbium doped fiber amplifiers," *IEEE Photon. Technol. Lett.*, vol. 2, 797 (1990).
- [15] H. Ono, M. Yamada, T. Kanamori, S. Sudo, and Y. Ohishi, "1.58- $\mu\text{m}$  Band Gain-Flattened Erbium-Doped Fiber Amplifier for WDM Transmission Systems," *J. Lightwave Technol.*, vol. 17, 490-496 (1999).
- [16] X. Y. Dong, P. Shum, N. Q. Ngo, H. Y. Tam, X. Y. Dong, "Output Power Characteristics of Tunable Erbium-Doped Fiber Ring Lasers," *J. Lightwave Technol.*, vol. 23, 1334-1341 (2005).
- [17] S. Q. Yang, C. L. Zhao, H. Y. Meng, L. Ding, X. O. Dong, S. H. Yuan, G. Y. Kai, and Q. D. Zhao, "Wavelength tunable erbium-doped fiber ring laser operating in L-band," *Opt. and Quantum Electron.*, vol. 35, 69-73 (2003).

# Chapter 4

## Wavelength-tuning mode-locked L-band erbium-doped fiber laser by controlled output-coupling-ratio

### 4.1 Introduction

Erbium-doped fibers (EDFs) covering optical gains in conventional and long wavelength bands have led to the realization of a broadband erbium-doped fiber amplifier (EDFA) for increasing the transmission capacity of a wavelength division multiplexing (WDM) communication system, and for developing and characterizing the fiber-optic devices with spectral bandwidth extended from C-band to L-band [1, 2]. For the needs of the next-generation time division multiplexing (TDM) system, an pulsed erbium-doped fiber laser (EDFL) with a tuning capability over the whole L-band needs to be developed. Various techniques have been proposed to realize the wavelength tuning or switching in mode-locked EDFLs by tuning the dispersion [3-7], by electrically controlling the delay time [8, 9], by changing the temperature of the Fabry-Perot laser diode (FPLD) modulator [10], by using an all-fiber based tunable filter [11, 12], and by changing wavelength-dependent cavity loss [13]. In this paper, we propose a novel scheme for wideband wavelength-tuning a mode-locked erbium-doped fiber-ring laser operated in L-band. Instead of changing polarization in the EDFL cavity, the wavelength-tuning is achieved by simply adjusting the output coupling ratio as well as the cavity loss of the EDFL. A tuning range of about 27.2 (1572.1 nm – 1599.3 nm) is obtained. During the wavelength tuning process, the

modulation frequency remains unchanged and the pulsewidth is less than 5 ps for each wavelength. Furthermore, nearly transform-limited EDFL pulses by linear compression with single mode fiber are generated.

## 4.2 Experimental setup

The experimental setup of the wavelength-tunable mode-locked EDFL is shown in Fig. 4.1. The optimized gain of the fiber laser is provided by an EDFA which is composed of two isolators, and a 30 m of highly doped erbium-doped fiber forward pumped with a 17.5-mW

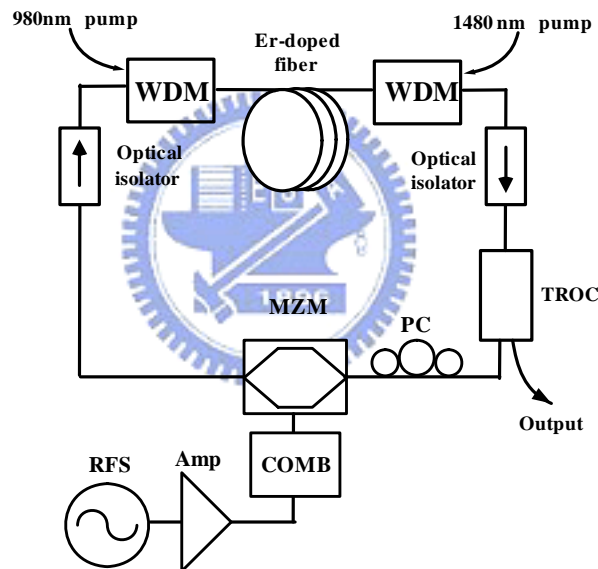


Fig. 4.1 Schematic diagram of the mode-locked EDFL with a TROC-based wavelength tuning configuration. Amp :power amplifier; COMB: comb generator; RFS: RF synthesizer; TROC: tunable ratio optical coupler; PC: polarization controller; MZM: Mach-Zehnder intensity modeulator

laser diode at 980 nm and backward pumped a 200-mW laser diode at 1480 nm. A  $\text{LiNbO}_3$  Mach-Zehnder intensity modulator (MZM) with a bandwidth of 1GHz is inserted into the EDFL cavity, which is then modulated by an amplified RF driven comb generator signal at 1 GHz for active mode-locking. Two optical isolators were

employed to ensure the unidirectional propagation and a polarization controller (PC) was need to optimize the polarization orientation of the circulating pulses. The output ratio of the EDFL is detuned by inserting a 1×2 tunable-ratio optical coupler (TROC) with a variable coupling ratio ranging from 0.5% to 99.5%. Note that there is no TBPF in the EDFL cavity for wavelength-tuning because the TROC adjusts different intracavity loss to detune the lasing wavelength. Besides, the characteristics of the output pulses are monitored by a digital sampling oscilloscope (Agilent 86110A + 86109A), an optical spectrum analyzer (OSA, Advantest Q8347) and a microwave spectrum analyzer (Agilent 8565E). The pulse duration is measured by an optical autocorrelator (Femtochrome, Fx-103p).

## 4.3 Results and Discussions

### A. *ML-EDFL with TBPF*

The total length of the L-band EDFL cavity is about 53 m, corresponding to a longitudinal mode spacing of 3.77 MHz. The active mode-locking is achieved by driving the MZM with a 17.5 dBm RF signal at a repetition frequency of 1 GHz, which is approximately the 270<sup>th</sup> harmonic of the fundamental longitudinal frequency of the EDFL cavity. The DC offset bias of the MZM is chosen to provide maximum extinction ratio of the electrical pulses, and the stable optical pulse is obtained by fine adjusting both of the polarization controller and the RF-driving frequency. Figure 4.2 shows the peak power and pulsewidth at 10%, 50%, and 90% output coupling ratio. A tuning range of about 45 nm (covering the whole L-band) for each output coupling ratio with different pulsewidth and peak power. In particular, the pulse-width becomes shortened as the output coupling ratio further decreases, and the shortest pulse-width of 8.8 ps is obtained at output coupling ratio of 10%.

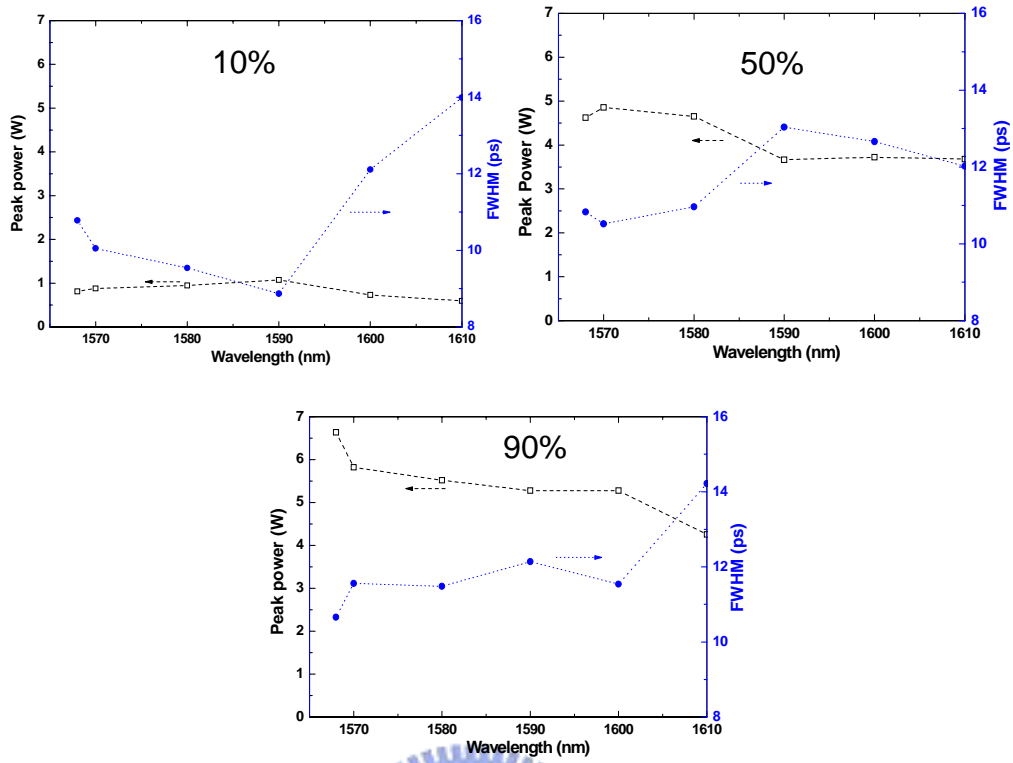
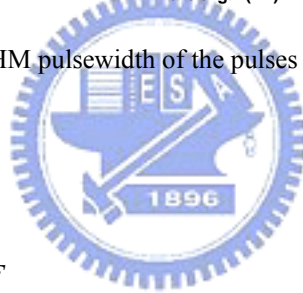


Fig. 4.2 The peak power and FWHM pulsedwidth of the pulses at output coupling ratio of 10%, 50%, and 90%.



### B. ML-EDFL without TBPF

The longitudinal mode spacing for the TBPF-free L-band EDFL is slightly enlarged to 3.922 MHz due to the removal of TBPF, while the active mode-locking is achieved at the 262<sup>th</sup> harmonic of the fundamental longitudinal frequency. Figure 4.3 shows the 3-dB spectral linewidth and central wavelength of the output spectra as the output coupling ratio is detuned from 10% to 90%.

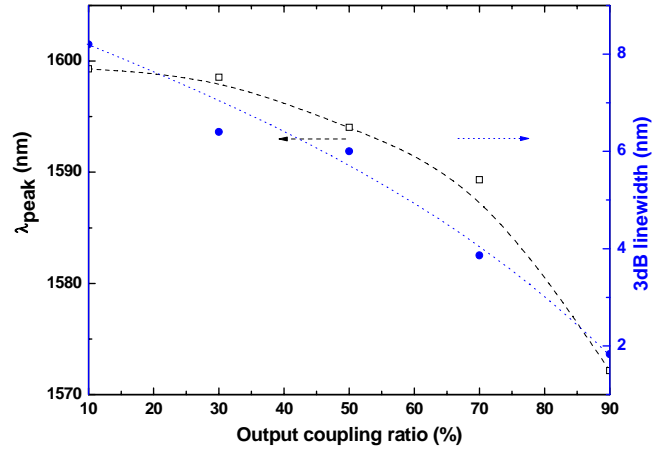


Fig. 4.3 The 3-dB spectral linewidth and central wavelength of the output EDFL spectra as the output coupling ratio detunes from 10% to 90%.

When the output coupling ratio decreases, the ASE obtains mostly gain of shorter wavelength and the lasing occurs at longer wavelength relatively. Furthermore, by decreasing the output coupling ratio from 90% to 10%, the wavelength can be tunable within a range of 27.2 nm (from 1572.1 nm to 1599.3 nm). According to the wavelength shifting phenomenon in Fig. 4.3, the wavelength should be tunable in the whole L-band as the output coupling ratio changes from 0.5% to 99.5%. The autocorrelation traces of the TBPF-free EDFL pulses illustrate that the pulsewidth shortens as the output coupling ratio decreases, which is mainly due to the broadening of the 3-dB spectral linewidth under an enlarged intra-cavity gain, is shown in Fig. 4.4.

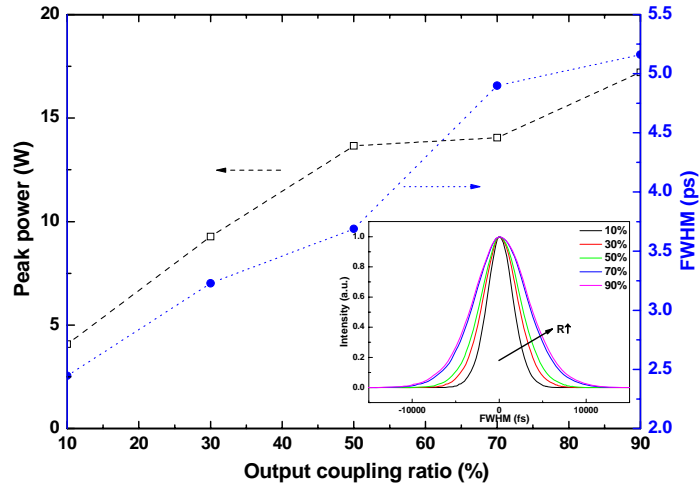


Fig. 4.4 The peak power and the pulsedwidth of the pulses as the output coupling ratio is adjusted from 10% to 90%. Inset: The autocorrelation traces of the output pulses.

In principle, the mode-locking pulsewidth is directly proportional with  $(g_0)^{1/4} / (\delta^2 \cdot f_m^2 \cdot \Delta\nu^2)^{1/4}$ , where  $f_m$  denotes the modulation frequency,  $\Delta\nu$  represents homogenous linewidth,  $g_0$  is single-pass integrated gain, and  $\delta$  denotes the on-to-off modulation depth. The narrowest pulsewidth of 2.4 ps with a largest 3-dB spectral linewidth of 8.2 nm is obtained at 1599.3 nm under a 10% output coupling ratio, providing a time-bandwidth product of 2.35 (Gaussian pulse shape assumed). In addition, the RF spectra of the EDFL pulse measured with a RBW of 10 Hz, a VBW of 10 Hz, and a frequency span of 10 MHz/div is demonstrated to show the ultrahigh supermode noise suppression ratio (SMSR) of more than 47 dB, as shown in Fig. 4.5. Such a high SMSR clearly indicates that the amplitude of the output pulses is very stable.



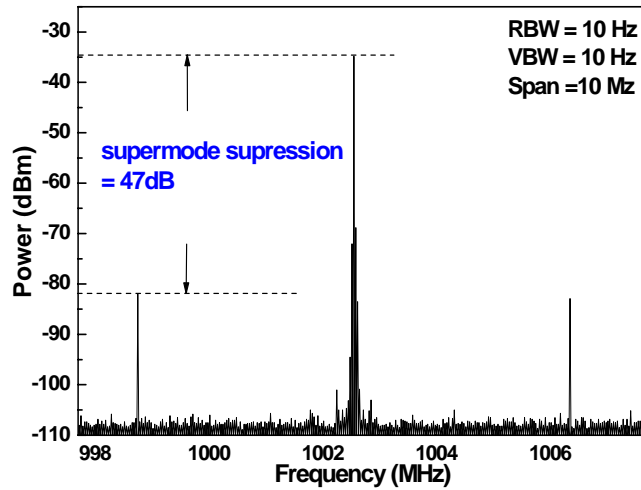


Fig. 4.5 RF spectrum of the output pulses at 1599.3 nm under 10% output coupling ratio.

### C. Linear compression of ML-EDFL without TBP

To obtain a narrow pulsewidth with a chirp-free property, the single-mode fiber (SMF) is added after the output port of the L-band ML-EDFL. Because the output pulse is positive chirped, the negative  $\beta_2$  value of the SMF is used to compress pulsewidth. Furthermore, from the unchanged shape of spectra before and after adding the SMF we can know that the dispersion compensation is linear, as shown in Fig. 4.6.

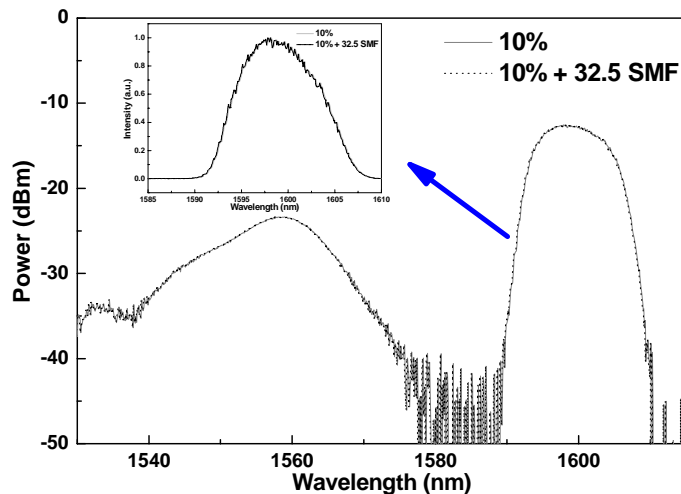


Fig. 4.6 Spectra before and after adding the SMF.

Figure 4.7 shows the shortening of pulsewidth after SMF with length changing from 22.5 m to 37.5 m. The narrowest pulsewidth of 580 fs fitted with Gaussian pulse is obtained with 32.5 m SMF, giving rise to a time-bandwidth product of 0.56. The obtained pulsewidth is shorter than those usually obtained from this the L-band EDFL configuration.

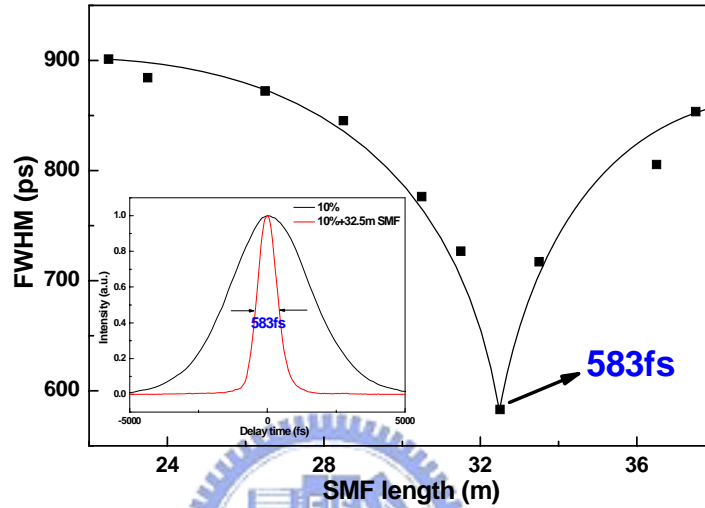


Fig. 4.7 Variation of pulsewidth by adding different length of the SMF from 22.5 m to 37.5 m. Inset: The autocorrelation traces of the output pulses before and after adding SMF at 10% output coupling ratio.

According to the theory of the optical pulse compression, if the leading edge of the pulse is delayed by just the right amount to arrive nearly with the trailing edge, the output pulse is compressed. Positively chirped pulses require anomalous or negative GVD in order to slow down the red-shifted leading edge [14]. In addition, the optimized linear compression is applied to the EDFL pulses obtained under different output coupling ratios, as shown in Fig. 4.8.

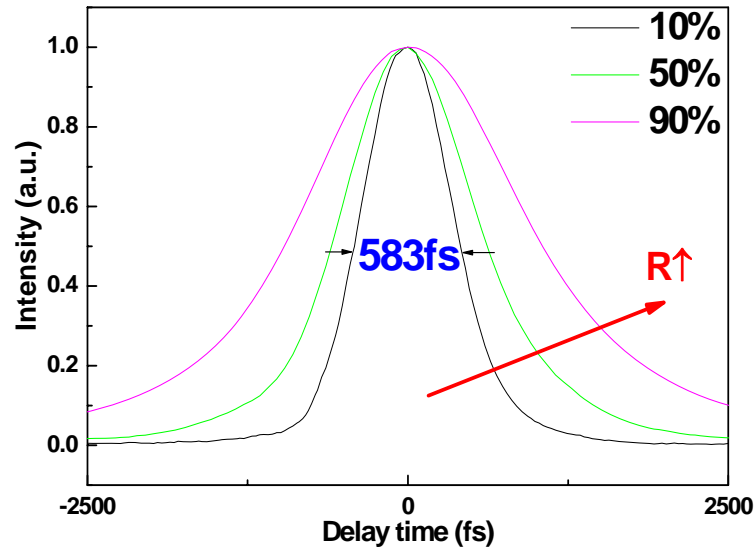


Fig. 4.8 The autocorrelation traces of the output pulses after adding 32.5 m SMF at 10%, 50%, and 90% output coupling ratio.

#### D. Comparison

Table 4.1 shows the wavelength tuning range, the narrowest pulsewidth, and the timing jitter of the L-band ML-EDFL with TBPF, TROC, and after linear dispersion compensation. Although the EDFL with a TBPF has larger wavelength tuning range, its pulsewidth is also broadened due to the finite spectral linewidth limited by the TBPF. The pulsewidth can be shortened if the TBPF is replaced by the TROC, in which the spectral linewidth becomes unlimited. Such a system therefore benefits from not only the simplified wavelength tuning technique but also the cost-effective solution to shorten the output pulsewidth.

Experimental setup	Tuning range (nm)	Pulsewidth (narrowest) (ps)	Jitter (ps)
with TPBF	45 (1567-1612)	8.8	1.4
without TBPF	27(1572-1599)	2.45	0.7
After compression	27(1572-1599)	0.58	0.7

Table 4.1 Comparison of the tuning range, the narrowest pulsewidth, and timing jitter in three different situations.

Previously, Duan et al. have demonstrated a stable dispersion-tuned harmonically mode-locked fiber ring (HMLFL) laser with a wavelength tuning from 1555.7 nm to 1568.1 nm and a pulse-width of 4 ps by using an intracavity semiconductor optical amplifier (SOA) as both a supermode-noise suppressor and a mode locker [3]. Chan et al. have proposed an EDFL that incorporates a SOA nonlinear fiber loop with a wavelength tuning from 1542.8 nm to 1562.3 nm and a pulsewidth of 30 ps by controlling the delay time between the modulation and the control signals in the compensated dispersion-tuning scheme [9]. Zhao et al. have demonstrated an EDFL with a wavelength tuning from 1546.6 to 1551.7 nm and a pulse-width of 51 ps by changing the FPLD temperature from 12.02°C to 19.65°C [10]. Jeon et al. have used an all-fiber acoustic-optic tunable filter to achieve a wavelength tuning from 1557 to 1607 nm and a pulsewidth of 1.5 ps [11]. In addition, Feng et al. have demonstrated a wavelength tuning range from 1568.6-1607.8 nm and a pulsewidth of <56 ps by adjusting an intracavity polarization controller to introduce wavelength-dependent cavity loss [13].

## 4.4 Conclusions

We have experimentally investigated an actively mode-locked EDFL, which is wavelength-tunable in L-band without using any intra-cavity bandpass filters. The wavelength tuning is achieved by adjusting the output coupling ratio of the EDFL with a TROC which introduces wavelength-dependent cavity loss as well as changing the peak of the gain profile. Using a TBPF facilitate a wider tuning range of 45 nm (covering the whole L-band) at a cost of a larger pulsewidth of 14.2 ps. In comparison, the TROC controlled EDFL exhibits a smaller tuning range of 27 nm and a shorter pulsewidth of <5 ps. Under the linear compression in a SMF, we

demonstrate the generation of nearly transform-limited Gaussian pulses with a peak power of 17 W and a pulsewidth of 580 fs at repetition rate of 1 GHz. These EDFL pulses are very stable with a side-mode suppressing ratio as high as 47 dB.

## 4.5 References

- [1] M. X. MA, M. Nissov, H. Li, M. A. Mills, G. Yang, H. D. Kidorf, A. Srivastava, J. Sulhoff, C. Wolf, Y. Sun, and D. W. Peckhan, “765 Gb/s over 2,000 km transmission using C- and L-band erbium doped fiber amplifiers”, Paper PD, OFC99, Feb. 1999, (San Diego, USA)
- [2] H. Ono, M. Yamada, T. Kanamri, S. Sudo, and Y. Ohishi, “1.58- $\mu\text{m}$  band gain-flattened erbium-doped fiber amplifiers for WDM transmission systems”, *J. Lightwave Technol.*, vol.17, pp.490-496, 1999.
- [3] L. Duan, M. Dagenais, and J. Goldhar, “Smoothly wavelength-tunable picosecond pulse generation using a harmonically mode-locked fiber ring laser”, *J. Lightwave Technol.*, vol. 21, pp. 930–937, 2003.
- [4] L. Duan, C. J. K. Richardson, Z. Hu, M. Dagenais, and J. Goldhar, “A stable smoothly wavelength-tunable picosecond pulse generator”, *IEEE Photon. Technol. Lett.*, vol. 14, pp. 840–842, 2002.
- [5] S. Li and K. T. Chan, “Electrical wavelength-tunable actively mode-locked fiber ring laser with a linearly chirped fiber Bragg grating”, *IEEE Photon. Technol. Lett.*, vol. 10, pp. 799–801, 1998.
- [6] J. He and K. T. Chan, “Generation and wavelength switching of picosecond pulses by optically modulating a semiconductor optical amplifier in a fiber laser with optical delay line”, *IEEE Photon. Technol. Lett.*, vol. 15, pp.798–800, 2003.
- [7] S. Li, K. T. Chan, H. Ding, and Z. Fang, “Electrical wavelength switching of

- mode-locked Er-doped fiber ring laser with two fiber gratings”, *Proc. Conf. Lasers Electro-Optics*, vol. 11, pp. 473–474, 1997.
- [8] K. Chan and C. Shu, “Electrical switching of wavelength in actively mode-locked fiber laser incorporating fiber Bragg gratings”, *Electron. Lett.*, vol. 36, pp. 42–43, 2000.
- [9] S. W. Chan and C. Shu, “Harmonically mode-locked fiber laser with optically selectable wavelength”, *IEEE Photon. Technol. Lett.*, vol. 14, pp. 771–773, 2002.
- [10] D. Zhao, K. T. Chan, Y. Liu, L. Zhang, and I. Bennion, “Wavelength-switched optical pulse generation in a fiber ring laser with a Fabry–Perot semiconductor modulator and a sampled fiber Bragg grating”, *IEEE Photon. Technol. Lett.*, vol. 13, pp. 191–193, 2001.
- [11] M.-Y. Jeon, H. K. Lee, J. T. Ahn, D. S. Lim, D. I. Chang, K. H. Kim, and S. B. Kang, “Wideband wavelength tunable mode-locked fibre laser over 1557–1607 nm”, *Electron. Lett.*, vol. 36, pp. 300–302, 2000.
- [12] S. Yang, Z. Li, X. Dong, S. Yuan, G. Kai, and Q. Zhao, “Generation of wavelength-switched optical pulse from a fiber ring laser with an F-P semiconductor modulator and a HiBi fiber-loop mirror”, *IEEE Photon. Technol. Lett.*, vol. 14, pp. 774–776, 2002.
- [13] X. Feng, Y. Liu, H. Zhang, Y. Li, S. Yuan, G. Kai, W. Zhang, and X. Dong, “Wide wavelength-switched optical-pulse generation in an L-band mode-locked erbium-doped fiber laser”, *Micro. and Opt. Technol. Lett.*, vol. 44, pp. 196–199, 2005.
- [14] G. P. Agrawal, *Nonlinear Fiber Optics* (Academic press, San Diego, 2001).

# Chapter 5

## Summary

### 5.1 Summary

First, we experimentally investigate and demonstrate the use of highly  $\text{Er}^{3+}$ -doped silica fiber as a L-band amplifier, obtaining in excess of 24.5 dB of small signal gain between 1560 nm and 1590 nm by forward pumping at 980 nm with power of 17.5 mW and backward pumping at 1480 nm with power of 200mW when the EDF length is 30 m. With such a simplified EDFA, an extremely high power conversion efficiency (PCE) of 37% with a wavelength dependent gain deviation of 6 dB is achieved. The high PCE shows more than 10% improvement as compared to that reported using conventional L-band EDFA configuration.

In second part, we experimentally investigated and demonstrated an output-coupling-ratio controlled, full long-wavelength-band erbium-doped fiber ring laser by using a bi-directionally dual-wavelength pumped EDFA which is talked in first part in close-loop with a tunable ratio optical coupler. The L-band EDFL is wavelength-tunable from 1567 nm to 1612 nm at a maximum quantum efficiency of 42%, respectively with ultra-high power conversion efficiency of 37%, comparable gain of 34 dB, and maximum output power of up to 91mW. The minimum wavelength tuning resolution of 0.3 nm is achieved under the maximum wavelength tuning range of up to 45 nm covering whole L-band, while a low channel power variation of <1.2dB and a stable output with 0.04% power fluctuation is observed.

Finally, we experimentally investigated an actively mode-locked erbium-doped fiber laser, which is wavelength-tunable in L-band without using any intra-cavity bandpass filters. The wavelength tuning is achieved by adjusting the output coupling ratio of

the EDFL with a TROC which introduces wavelength-dependent cavity loss as well as changing the peak of the gain profile. Using a TBPF facilitate a wider tuning range of 45 nm (covering the whole L-band) at a cost of a larger pulse-width of 14.2 ps. In comparison, the TROC controlled EDFL exhibits a smaller tuning range of 27 nm and a shorter pulse-width of  $<5$  ps. Under the linear compression in a SMF, we demonstrate the generation of nearly transform-limited Gaussian pulses with a peak power and a pulsewidth of 17 W and 583 fs, respectively at repetition rate of 1 GHz. These EDFL pulses are very stable with a side-mode suppressing ratio as high as 47 dB.





# 作者簡介

姓名：張峻源

出生地：台灣省台北市

出生日期：70/11/01

學歷：台南市崇學國民小學  
台北市私立方濟國民中學  
台北市立建國中學  
國立交通大學電子物理系  
國立交通大學光電工程研究所

專長：摻鉕光纖放大器  
摻鉕光纖雷射  
主動可調波長鎖模光纖雷射  
拉曼放大器  
摻鉕光纖放大器的基本特性分析



國際期刊論文與研討會論文投稿及發表紀錄：

期刊：

1. **Jun-Yuan Chang**<sup>1</sup>, Hai-Han Lu<sup>2</sup>, and Gong-Ru Lin<sup>1\*</sup>, “A Coupler and Air-Gap Etalon Controlled High-Efficiency L-Band Erbium-Doped Fiber Laser”, *IEEE Photon. Technol. Lett.* (Revised, June, 2006).

研討會：

1. **Jun-Yuan Chang**, Yu-Sheng Liao<sup>1</sup>, Chi-Ming Hung<sup>1</sup>, Hai-Han Lu<sup>2</sup> and Gong-Ru Lin<sup>1\*</sup>, "A Power Conversion Efficiency Improved L-Band Erbium-Doped Fiber Laser with Coupling-Ratio Controlled Wavelength Tunability", *Conference of Optics and Photonics/Taiwan'(OPT) 05*, paper, Taipei, Taiwan, December 9-10, 2005



